Multi-objective Power Flow Optimization Based on Improved Hybrid Crow Search Algorithm: A Novel Approach

Gonggui Chen, Xiang Wang, Shuangjin Mo, Jian Zhang, Wei Xiong, Hongyu Long* and Mi Zou

Abstract—**An improved hybrid crow search algorithm (IHCSA), whose purpose is to find the best measured solution (BMS), is proposed to solve the multi-objective optimal power flow (MOOPF) problem. The proposed IHCSA, which creatively combines the advanced ideas and strategies of sinusoidal nonlinear dynamic transformation awareness probability (SNDTAP) and tent map switching fly length (TMSFL), introducing the mutation and crossover processes of differential evolution (DE), obtains a better BMS. Three innovative optimization strategies are integrated into this paper. The proposed screening approach of Pareto-priority mechanism (SAPM) ensures that the state variables meet the inequality constraints of power systems. The Pareto optimal set (POS) is obtained by elite non-dominant sorting method (ENSM). Besides, the BMS, obtained by fuzzy membership theory, is filtered from POS. For practical purposes, five objective functions are considered. Three various scale test systems are applied to validate the performance of the IHCSA. Simulation results reveal that the proposed method has a greater competitive advantage in addressing non-convex MOOPF problems of different scales. In addition, Hypervolume (HV) and Spacing (SP) are used to quantitatively evaluate the diversity and consistency of POS gained by IHCSA. The evaluation results prove that the proposed approach has excellent performance and great application prospects.**

Index Terms—**Improved hybrid CSA, optimal power flow, optimization strategies, performance evaluation indexes**

Manuscript received May 25, 2022; revised September 23, 2022. This work was supported by the National Natural Science Foundation of China (52007022), the Project funded by the China Postdoctoral Science Foundation(2021M693930).

Gonggui Chen is a professor of Key Laboratory of Industrial Internet of Things and Networked Control, Ministry of Education, Chongqing University of Posts and Telecommunications, Chongqing 400065, China (e-mail: chenggpower@163.com).

Xiang Wang is a graduate student of Chongqing University of Posts and Telecommunications, Chongqing 400065, China (e-mail: 15730695224@163.com).

Shuangjin Mo is a marketing director of State Grid Chongqing Qianjiang Power Supply Company, Chongqing, 409000, China (e-mail: moshuangjin_qj@163.com).

Jian Zhang is an engineer of State Grid Chongqing Qianjiang Power Supply Company, Chongqing, 409000, China (e-mail: zhangjian_qj@163.com).

Wei Xiong is an assistant engineer of State Grid Chongqing Qianjiang Power Supply Company, Chongqing, 409000, China (e-mail: xiongwei_qj@163.com).

Hongyu Long is a professor level senior engineer of Chongqing Key Laboratory of Complex Systems and Bionic Control, Chongqing University of Posts and Telecommunications, Chongqing 400065, China (corresponding author to provide phone: +8613996108500; e-mail: longhongyu20@163.com).

Mi Zou is an assistant professor of Chongqing Key Laboratory of Complex Systems and Bionic Control, Chongqing University of Posts and Telecommunications, Chongqing 400065, China (e-mail: zoumi@cqupt.edu.cn).

I. INTRODUCTION

OPTIMAL power flow (OPF), an optimization technique that has received extensive attention in power system research., must ensure the safety of the system operation when adjusting control variables and meet the physical constraints simultaneously. The purpose is to obtain an ideal operation state for the system[1]. The crux of the matter is that OPF cannot be put into a continuous mathematical model for the solution, which is one of the several difficulties in practical engineering projects[2].

Since the 21st century, the use of electric energy has been further enhanced, and the task of the electric power system has become more onerous. How to better plan and optimize the electric power system has attracted the attention of researchers[3,4]. In previous studies, the OPF problem is mainly concerned with minimizing fuel cost, emission, and active power loss, respectively. To measure the running state of the power system comprehensively and meet the needs of the actual system, the research often considers multiple optimization objectives in an integrated manner. The multi-objective uncoordinated constraint problem in the power system is called the multi-objective optimal power flow problem (MOOPF)[5].

The MOOPF problem, which has non-convex and high dimensional characteristics, optimizes the given targets by tailoring the control variables to meet various constraints. Unlike the search for a single optimal decision, the MOOPF attempts to calculate a set of control schemes, and, ultimately, the best-measured solution (BMS).

Previously, classical methods were to assign different weights to each objective in dealing with the MOOPF problem based on decision-makers' priorities and solutions. However, traditional methods also inevitably have some defects. For example, the conventional approach is not suitable for the unknown situation of decision-makers. For high-dimensional problems such as MOOPF, it is almost impossible to find POS in a complex system[6]. Therefore, the use of other feasible ways to deal with the MOOPF problem deserves to be developed vigorously[7-11].

Throughout the years, breakthroughs and innovations in computer technology have provided a solid foundation for the growth of heuristic algorithms lately[12-19]. Many researchers have made much progress in solving the MOOPF problem with heuristic algorithms[20-23]. For instance, BP neural network is introduced to predict the latent schemes around BMS [24]. A method called Manta ray foraging optimization is used to find feasible solution sets[25]. In literature [26], a multi-objective optimizer NSWOA was applied to multiple engineering problems. In literature [27], a dimension-based firefly algorithm obtains POS with high-quality effects. A hybrid firefly-bat algorithm is introduced to enhance the population diversity in [28]. The modified beetle antennae search algorithm and BP are applied to solve the MOOPF problem in [29]. In literature [30], a multi-objective optimization approach is introduced to resource management of heterogeneous cellular networks. The results reveal that applying the heuristic algorithm to solve the MOOPF problem is very effective.

Crow search algorithm (CSA) is a new intelligent optimization algorithm developed recently. It was proposed by Askarzadeh in 2016[31]. Due to its relatively simple structure and few key parameters, CSA has been widely used in different fields[32-36]. Nevertheless, the original CSA is still prone to fall into local optimization and lack diversity[37].

In order to solve the MOOPF problem, this paper proposes an improved hybrid crow search algorithm (IHCSA) with sinusoidal nonlinear dynamic switching awareness probability and tent map switching flight length, combined with the variation and crossover process model of the differential evolution (DE) algorithm. To evaluate the practicability of IHCSA, several research cases were selected to test it on IEEE30-, 57-, and IEEE118-bus systems and the test results are more accurate than those of recent literature, highlighting IHCSA's applicability and core competencies.

The rest of article is structured as follows: The mathematical model in the area of MOOPF is depicted in Section II. The strategies to solve the MOOPF problem are given in Section III. The IHCSA's application in MOOPF is described at Section IV. In addition, Section V represents simulation study and scenario analysis of ten different research components. Finally, the performance evaluation index data are obtained at Section VI. Section VII summarizes this work.

II. MOOPF Mathematical Model

The MOOPF problem model contains the examination and optimization of different combinations of objectives. At the same time, various constraints of the system must be included in the scope of restrictions[38]. The components of the MOOPF mathematical model are described in detail as the following:

$$Min\ S_{obj}(x,u)=\{S_1(x,u),\cdots,S_i(x,u),\cdots,S_m(x,u)\} \quad (1)$$

$$H_k(x,u)=0,\quad k=1,\cdots,k,\cdots,H_{length} \quad (2)$$

$$G_j(x,u)\le 0,\quad j=1,\cdots,j,\cdots,G_{length} \quad (3)$$

where $S_i(x,u)$ represents the ith objective function that needs to be optimized, and m is the target number. $H_k(x,u)$ denotes the kth equality constraint and $G_j(x,u)$ describes the jth inequality constraint. H_{length} and G_{length} depict the amount of equality restraints and inequality restraints, separately.

$$x^T=\left[P_{Gen1},V_{L1},\cdots,V_{LC_{PQ}},Q_{Gen1},\cdots,Q_{GenN_G},S_{TL_1},\cdots,S_{TL_{CTL}}\right] \quad (4)$$

where x is defined as the vector of state variables, which incorporates a large variety of variables. Active power output of generator at slack bus P_{Gen1}, which regulates the system output. V_L, load bus voltage, must not cross the line voltage carrying range. Generator reactive power Q_{Gen}, which cannot be ignored. The apparent power of transmission line S_{TL} is also in the scope of consideration.

u is a vector of control variables, which incorporates many control points. The tap setting of the transformers T is considered. Active power output of generators other than P_{Gen1}, is the main source of energy for the system. The voltage magnitude of generators V_{Gen}, reflects, to some extent, the generator operating condition. The injected reactive power of shunt compensators Q_C, enables the system network to work better. It can be described as:

$$u^T=\left[P_{Gen2},\cdots,P_{GenN_G},V_{Gen1},\cdots,V_{GenN_G},T_1,\cdots,T_{N_T},Q_{C_1},\cdots,Q_{C_{N_C}}\right] \quad (5)$$

where C_{PQ} signifies the count of load buses, and N_G depicts the number of generators. CTL is the count of transmission lines. N_T and N_C denote the number of transformers and shunt compensators.

A. Objective Functions

This paper will optimize the five objective functions, including basic fuel cost, fuel cost with value-point, emission, voltage deviation, and active power loss. The specific groups can be seen in TABLE II.

1) S_{fcost}

$$S_{fcost}=\sum_{i=1}^{N_{Gen}}(Ca_i+Cb_iP_{Geni}+Cd_iP_{Geni}^2)\ \$/\mathrm{h} \quad (6)$$

where S_{fcost}, basic fuel cost, depicts one of the main costs. Ca_i, Cb_i and Cd_i are the cost coefficients.

2) $S_{emission}$

$$S_{emission}=\sum_{i=1}^{N_{Gen}}[\alpha_iP_{Geni}^2+\beta_iP_{Geni}+\zeta_i+\eta_i\exp(\lambda_iP_{Geni})]\ \mathrm{ton/h} \quad (7)$$

where $S_{emission}$ represents the total emissions. α_i, β_i, γ_i, ζ_i, and λ_i , emission factors, are some real numbers.

3) S_{Ploss}

$$S_{Ploss}=\sum_{k=1}^{N_{TL}}G_k[V_i^2+V_j^2-2V_iV_j\cos(\delta_i-\delta_j)]\ \mathrm{MW} \quad (8)$$

where S_{Ploss} depicts the active power loss. G_k depicts the conductance of branch k. V_i and V_j refer to the voltage magnitude at bus i and j. δ_i and δ_j describe voltage angle at bus i and j, respectively.

4) S_{fcost_vp}

$$S_{fcost\_vp}=\sum_{i=1}^{N_G}[a_i+b_iP_{Gen_i}+c_iP_{Geni}^2+ \left|d_i\sin(e_i(P_{Geni}^{\min}-P_{Geni}))\right|]\ \$/\mathrm{h} \quad (9)$$

where S_{fcost_vp} depicts the fuel cost with value-point loadings. d_i and e_i depict cost coefficients. $P_{Geni}^{\min}$ denotes lower active power, which is valid for the ith generator.

5) S_{VD}

Voltage deviation reflects the quality of the electrical energy in the line and its magnitude directly influences the power system's stability and economic benefit. It can be written as below:

$$S_{VD}=\sum_{nu=1}^{N_{PQ}}|V_{nu}-1| \quad (10)$$

where S_{VD} denotes the total voltage deviation of a system.

B. Variable Constraints

Only when the power system's all constraints are satisfied simultaneously does the optimization of five objective functions have practical significance.

1) Equality Constraints

The equality constraints reveal elegantly load flow equations, whose connotations are depicted below:

$$P_{Gi} = P_{Di} + V_i \sum_{j=1}^{Nb_i} V_j (G_{ij} \cos(\delta_i - \delta_j) + B_{ij} \sin(\delta_i - \delta_j)), \forall i \in NB \quad (11)$$

$$Q_{Gi} = Q_{Di} + V_i \sum_{j=1}^{Nb_i} V_j (G_{ij} \sin(\delta_i - \delta_j) - B_{ij} \cos(\delta_i - \delta_j)), \forall i \in N_{PQ} \quad (12)$$

where P_{Gi} and Q_{Gi} denote the injected active and reactive power at generator bus i while P_{Di} and Q_{Di} depict the active and reactive load demand at load bus i. In addition, G_{ij} and B_{ij} signify the conductance and susceptance, respectively. Nb_i depicts the count of the buses contiguous with bus i, including bus i; NB is the amount of system buses other than the slack bus; N_{PQ} indicates the amount of PQ buses.

2) Inequality Constraints

System variables need to be restricted to valid ranges, inequality constraints involve constraints of state variables and control ones[28].

(1) Inequality constraints of control variables

(i) Active Power P_G Constraints

$$\begin{matrix} P_{Geni}^{\max} - P_{Geni} \geq 0 \\ P_{Geni} - P_{Geni}^{\min} \geq 0 \end{matrix}, \; i \in N_G (i \neq 1) \quad (13)$$

(ii) Voltage V_G Constraints

$$\begin{matrix} V_{Geni}^{\max} - V_{Geni} \geq 0 \\ V_{Geni} - V_{Geni}^{\min} \geq 0 \end{matrix}, \; i \in N_G \quad (14)$$

(iii) Transformer Tap-settings T Constraints

$$\begin{matrix} T_i^{\max} - T_i \geq 0 \\ T_i - T_i^{\min} \geq 0 \end{matrix}, \; i \in N_T \quad (15)$$

(iv) Reactive Power Sources Q_C Constraints

$$\begin{matrix} Q_{Ci}^{\max} - Q_{Ci} \geq 0 \\ Q_{Ci} - Q_{Ci}^{\min} \geq 0 \end{matrix}, \; i \in N_C \quad (16)$$

(2) Inequality constraints of state variables

(i) limitations for P_{Gen1}

$$\begin{matrix} P_{Gen1}^{\max} - P_{Gen1} \geq 0 \\ P_{Gen1} - P_{Gen1}^{\min} \geq 0 \end{matrix} \quad (17)$$

(ii) restrictions on voltages at load buses

$$\begin{matrix} V_{Li}^{\max} - V_{Li} \geq 0 \\ V_{Li} - V_{Li}^{\min} \geq 0 \end{matrix}, \; i \in N_{PQ} \quad (18)$$

(iii) restrictions on generator reactive power

$$\begin{matrix} Q_{Geni}^{\max} - Q_{Geni} \geq 0 \\ Q_{Geni} - Q_{Geni}^{\min} \geq 0 \end{matrix}, \; i \in N_G \quad (19)$$

(iv) restrictions on apparent power

$$S_{ij}^{\max} - S_{ij} \geq 0, \; ij \in N_{TL} \quad (20)$$

III. Multi-objective Problem Processing Strategy

In order to choose the most suitable BMS for the current situation among many alternatives, three multi-objective strategies are taken into adoption.

A. Constrained Preemptive Strategy

It can be obtained from the Newton-Raphson power flow calculation whether the *i*th individual violates the equality constraints. Moreover, the control variables of the *i*th crow could be depicted in (21).

$$u_i = \begin{cases} u_i^{\max} & if \; u_i > u_i^{\max} \\ u_i^{\min} & if \; u_i < u_i^{\min} \\ u_i & otherwise \end{cases} \quad (21)$$

Given the inequality constraint treatment of state variables, a screening approach of the Pareto-priority mechanism (SAPM), which is significantly different from the traditional penalty coefficient method, is proposed to solve this problem. Its main steps are as follows:

(i) Calculate the violation of inequality constraints for *i*th individual $viol(u_i)$ (22).

$$sum\_viol(u_i) = \sum_{j=1}^{H_s} \max(G_j(x, u_i), 0) \quad (22)$$

where H_S represents the count of inequality constraints on the state variables.

(ii) u_1 and u_2, two different control variables, are selected randomly, and their violations are compared. When the formula (23) is satisfied, u_1 is dominant u_2.

$$sum\_viol(u_1) < sum\_viol(u_2) \quad (23)$$

(iii) If any of the conditions (24) and (25) are satisfied, it means that u_1 is dominant u_2. u_1 is regarded as a Pareto non-dominated solution.

$$sum\_viol(u_1) = sum\_viol(u_2) \quad (24)$$

$$\begin{cases} S_i(x, u_1) \leq S_i(x, u_2), \; \forall i \in \{1, 2, ..., m\} \\ S_j(x, u_1) < S_j(x, u_2), \; \exists j \in \{1, 2, ..., m\} \end{cases} \quad (25)$$

B. Elite Non-dominated Sorting Method

To obtain the uniformly distributed Pareto front, this paper adopts an elitist non-dominated ranking method first proposed by Deb in 2002[39]. The proposed Pareto dominant rule determines two attributes of each individual.

C. Rank and Density Calculation

1) Rank

It is assumed that each crow individual i in the crow population has two parameters: $C_o(i)$ and $C_m(i)$. $C_o(i)$ depicts the amounts of crows dominated crow i, and $C_m(i)$ represents the number of individuals dominated by individual i. The rules for determining the rank are described as follows:

Step1: Find all crows i with $C_o(i)$=0, place them in set P, and mark them as $Rank$=1.

Step2: For each individual crow k in the current set P, we probe into the number of crow individual $C_m(k)$ it dominated. If $C_o(k)$=1, then we put crow individual k into another set Q, and mark them as $Rank$=2.

Step3: Repeat step1 and step2 until all crows have their rank.

2) Density Calculation

Evaluation of a collection of multiple programs, the crowding distance, can be obtained by calculating the average distance between each adjacent two positions in the collection.

Density Calculation of the *i*th crow can be defined as below:

$$D_{calculation}(i)=\sum_{j=1}^{NS}\frac{S_j(i-1)-S_j(i+1)}{S_j^{\max}-S_j^{\min}} \tag{26}$$

where NS is the number of objective functions. In addition, S_j^{max} and S_j^{min} indicate the jth goal's upper and lower boundary values.

It is used to distinguish the order between multiple Pareto solutions in the same hierarchy, with the solution with the highest number being considered the manager's preferred solution. This is because solutions with larger values are more applicable.

D. Best-Measured Solution Based on Fuzzy Affiliation Rule

We are able to obtain multiple solutions with the same priority by the previous method, but we cannot objectively select from them the individual that is applicable at a given moment. A solution, which is determined quickly and objectively and meets the scheduler's current requirements, is called the best-measured solution (BMS).

The following two formulas describe in detail the basis for BMS selection. $F_{i,k}$ depicts satisfaction of the ith goal for the kth crow.

$$F_{i,k}=\begin{cases}1 & S_i\le S_i^{\min}\\ \dfrac{S_i^{\max}-S_i}{S_i^{\max}-S_i^{\min}} & S_i^{\min}<S_i<S_i^{\max}\\ 0 & S_i\ge S_i^{\max}\end{cases} \tag{27}$$

$$i=1,2,\dots NS \quad k=1,2,\dots,NP$$

$$Sat(k)=\frac{\sum_{i=1}^{NS}F_i\ (k)}{\sum_{k=1}^{NP}\sum_{i=1}^{NS}F_i\ (k)} \tag{28}$$

where the $Sat(k)$ represents the superiority of the kth solution, the BMS achieved by the rule has the highest satisfaction. NP is the size of POS.

IV. Improved and Hybrid Approach

The original crow search algorithm only has two main parameters, awareness probability (AP) and flight length (fl), which are simple and flexible. It has been applied to many interesting areas and projects.

However, the original CSA is still prone to fall into local optimization and lacks enough diversity. An improved hybrid crow search algorithm is proposed to aim at the above shortcomings.

A. Standard Crow Search Algorithm

The crow search algorithm was proposed by Askarzadeh in 2016 and applied to engineering design problems[31]. It is a new optimization algorithm proposed by imitating the intelligent behavior of crows when they store and steal food.

The search process of the crow search algorithm is controlled by two parameters: awareness probability (AP) and flight length(fl). If the random number *rand* is bigger than AP, the crow is closer to the memory location of the hidden food. Otherwise, the crow will choose a random location in the search space to deceive the stalker. The formula can describe the search process(29):

$$C_i(k+1)=\begin{cases}C_i(k)+r_j\times fl(k)\times(M_j(k)-C_i(k))\ if\ r_i\ge AP_j\\ a\ rand\ \ position \qquad\qquad otherwise\end{cases} \tag{29}$$

where $C_i(k)$ is the position of crow i at iteration k. $M_j(k)$ is crow j's memory of hiding food location at the current iteration. r_i and r_j are two stochastic data in [0,1]. AP_j is the awareness probability of crow j. Related research clearly depicts that fl works for most problems when it is 2.

B. The IHCSA

Three methods are proposed to amend the standard CSA, SNDTAP, TMSFL and SAPM.

1) Sinusoidal Nonlinear Dynamic Transforming Awareness Probability

For the normative CSA, Askarzadeh believes it can achieve strong applicability and processing accuracy when AP is 0.1. However, some researches reveal that sinusoidal nonlinear dynamic switching awareness probability. SNDTAP is proposed to makes AP more dynamic and effective, which could be defined as below:

$$AP=AP_{\min}+(AP_{\max}-AP_{\min})\sin(\frac{\pi}{2}\frac{k}{K_{\max}}) \tag{30}$$

where $AP_{\max}$ and $AP_{\min}$ are set as 0.5 and 0.01, representing the maximum and minimum values of awareness probability, respectively.

2) Tent Map Switching Fly Length

fl is usually set as 2 in the standard CSA. According to the algorithm's principle, fl will affect the flight distance of crows, affecting the global search and local search ability of CSA. To improve the global and regional random traversal capability of the algorithm search, the tent map method is introduced to make fl switch dynamically along with the iterative process, and its transformation process can be understood as follows:

$$fl(k+1)=\begin{cases}\dfrac{fl(k)}{\alpha} & fl(k)<\alpha\\ \dfrac{1-fl(k)}{1-\alpha} & fl(k)\ge\alpha\end{cases} \quad \alpha\in(0,1) \tag{31}$$

where $fl(k)$ represents the size when the number of iterations is k. As shown in the literature [37], α is set as 0.7.

3) Mutation and Crossover Operation of DE

The crow search algorithm cooperates with global and local search. The mutation crossover mechanism of the DE algorithm is embedded in CSA method, which improves the CSA's ability to jump out of local optimal and enhances the diversity of the original crow search algorithm.

Meanwhile, it is also helpful to improve its local search capability of CSA. The mutation updating way of DE algorithm is as below:

$$\begin{aligned}&M\_C(k+1)=C_{r1}(k)+F_c(C_{r2}(k)-C_{r3}(k))\\ &r_i\in[1,NP] \qquad i=1,2,3\end{aligned} \tag{32}$$

where $M\_C(k+1)$ is a new crow created by a mutation mechanism. C_{r1}, C_{r2}, and C_{r3} are the three crows randomly selected from the crow population in the current iteration. r_1, r_2, and r_3 are three different random numbers. F_c, a fundamental constant, denotes a variable scaling factor that controls the variation process.

The search and update approach corresponding to the crossover process is as below:

$$C_{i,d}(k+1)=\begin{cases} M\_C_{i,d}(k+1), & if\ rand(0,1)\le CR\ or\ d=d_{rand} \\ C_{i,d}(k), & otherwise \end{cases}$$
$$d=1,\cdots,d,\cdots,D_{cv} \tag{33}$$

where, D_{cv} represent the dimensions of control variables. d depicts d-th control variables. Besides, CR, the crossover factor, usually doesn't exceed 1. It's a real constant. D_{rand} is a random number from 1 to D_{cv}.

The pseudo-code of IHCSA is succinctly described in TABLE I.

TABLE I
PSEUDO CODE OF IHCSA

Input: $S_{obj}(x,u)=\{S_1(x,u),..., S_i(x,u),…, S_m(x,u),\}$
The crow group is stochastically initialized. under system constraints. Set relevant parameters of the IHCSA algorithm: crow population NP, awareness probability AP, flight length fl, maximum iteration K_{max}, etc.
Begin
k=0;
while ($k < K_{max}$)
Dynamically update AP by formula (30);
fl is updated randomly by formula (31);
for ith crow (i=1, …, N_a)
Generate two random numbers named $rand1$ and $rand2$.
if $rand1>AP$
According to the formula (29) and (32), a global jump search is performed;
else
for j=1, 2, …, N_{CV} (The dimension of crow individual)
if $rand2<CR \,\|\, d<d_{rand}$
Update the j-th position of crow i according to the formula (33);
end
end
end
end
Renovate the optimal global information;
k++;
end
End
output: BMS and Other alternatives;

V. SIMULATION RESULT

To validate IHCSA's processing capabilities., the way's performance was tested in IEEE30-, IEEE57-, and IEEE118-bus systems. TABLE II lists ten different cases which need to be handled.

The steps of the MOOPF problem with the IHCSA method are illustrated in Fig. 3. Also, basic codes of three optimization ways are implemented in MATLAB R2019a software in a PC with Intel(R) Core (TM) i5-7400CPU @3.00GHz with 16GB RAM.

A. Test Systems

An IEEE30-bus system, whose structure is shown in Fig. 1. The main parameters include 6 generators and 30 buses. The upper and lower limitations of taps of 4 transformers are 1.1p.u. and 0.9p.u.

Detailed data on the correlation coefficient could be obtained in [28]. The generators and load buses are given, whose voltage variation ranges are 0.95 to 1.1 p.u.

Does Fig. 2 describes the main features of the IEEE57-bus system, whose detailed data are given in the literature [27,28].

Transformer taps are between 0.9 and 1.1 p.u, shunt capacitors are limited between 0 and 0.3p.u.

Meanwhile, voltage amplitudes of PQ and PV busbars are determined in [0.9, 1.1] p.u, including a set of 33-dimensional control variables.

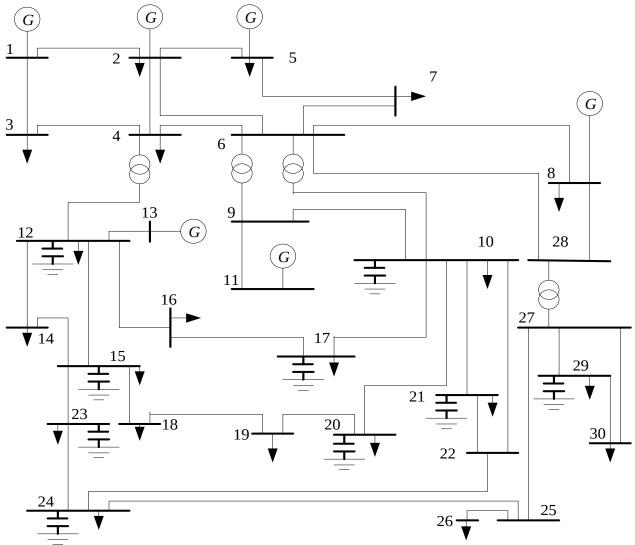

Fig. 1.The internal distribution of IEEE 30

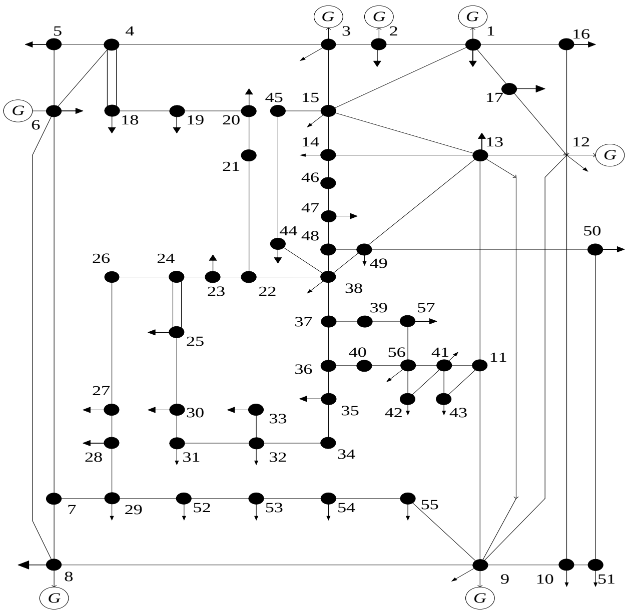

Fig. 2.The internal distribution of IEEE 57

A larger scale IEEE118-bus system will be applied to comprehensively evaluate the properties of IHCSA to deal with the MOOPF problem in a complex system.

Does Fig. 4 shows a single wireframing diagram of the IEEE118-bus system with 128-dimensional vectors.

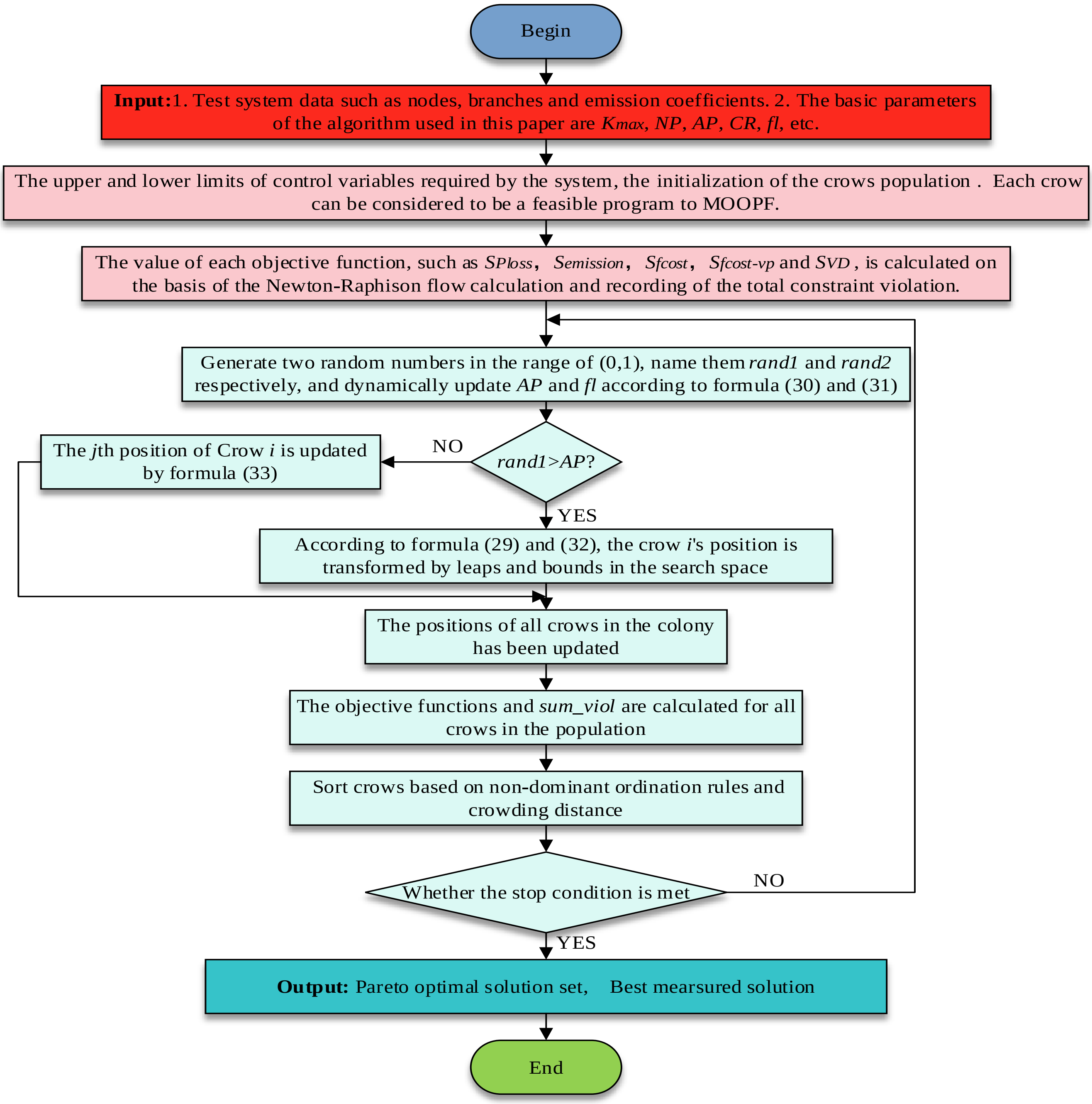

Fig. 3. The steps of the MOOPF problem with the IHCSA method

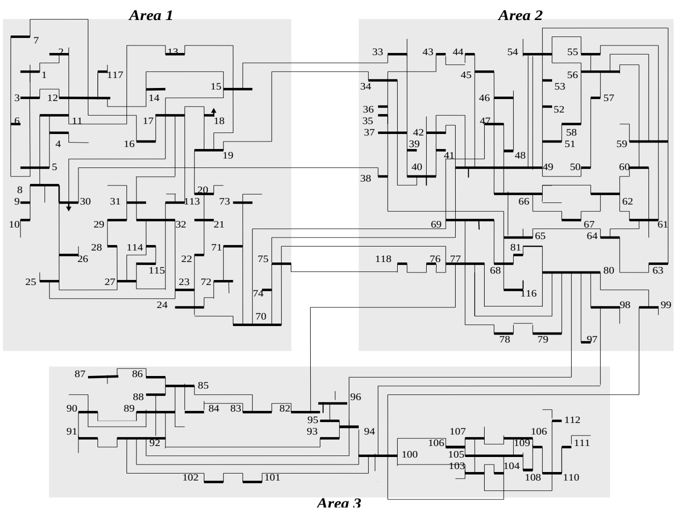

Fig. 4.The internal distribution of IEEE 118

TABLE II
OBJECT OF CASES

	S_{fcost}	$S_{emission}$	S_{Ploss}	$S_{fcost\text{-}vp}$	S_{VD}	Test System
Case1	✔		✔			IEEE30
Case2	✔	✔				
Case3			✔	✔		
Case4	✔				✔	
Case5	✔	✔	✔			
Case6		✔	✔			
Case7	✔		✔			IEEE57
Case8	✔	✔				
Case9	✔		✔			IEEE118
Case10	✔	✔				

The *PV* bus voltage amplitude limit is the same as that of IEEE 57, and other detailed parameters of the IEEE118-bus system can be obtained in [28].

TABLE III
DETAILED PARAMETERS OF THE ALGORITHM

Methods	Parameters	Case1-6	Case7-8	Case9-10
IHCSA	Population Size *NP*	100	100	100
	Maximum Iteration K_{max}	300	500	500
	Awareness Probability AP_{max}/AP_{min}	0.5/0.01	0.5/0.01	0.5/0.01
	fly length *fl*	0.8	0.8	0.8
	Zoom Scaling factor *Fc*	0.6	0.6	0.6
	Crossed factor *CR*	0.8	0.8	0.8
CSA	Population Size *NP*	100	100	-
	Maximum Iteration K_{max}	300	500	-
	Awareness Probability *AP*	0.1	0.1	-
	fly length *fl*	2.0	3.5	-
MOPSO	Population Size *NP*	100	100	-
	Maximum Iteration K_{max}	300	500	-
	Learning factor *c1*/*c2*	2/2	2/2	-
	Inertia weight factor w_{max}/w_{min}	0.9/0.4	0.9/0.4	-
NSGA-II	Population Size *NP*	100	100	100
	Maximum Iteration K_{max}	300	500	500
	Mutation index/percentage	20/0.1	20/0.1	20/0.1
	Crossover index/percentage	20/0.1	20/0.1	20/0.1

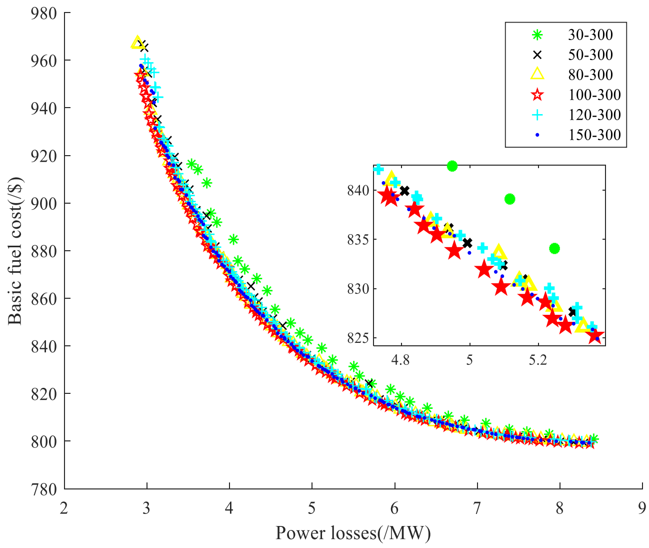

Fig. 5.PFs in different population sizes (K_{max} = 300)

B. Algorithm Parameters

Considering the population size and the maximum number of iterations, a simulation experiment, which takes the cost of basic cost and power loss as objective functions, is carried out in the IEEE30-bus system to explore the influence of IHCSA. Fig. 5 reveals that IHCSA obtains the PFs in different population sizes under the same iteration number of 300.

As can be seen from Fig. 5, IHCSA can obtain relatively evenly distributed PFs when the population size is [30, 50, 80, 100, 120, 150]. It indicates that the IHCSA proposed in this paper can have a positive optimization effect on different scale of groups. That is, we can flexibly adjust the population size in practical application scenarios and use X for optimality search. Generally, when the population size is 100 and 150, the optimization effect of the IHCSA algorithm is more prominent. Considering the impact of running time, the crow population size is set as 100 in all experiments conducted in this paper. In addition, the performance of IHCSA under various K_{max} is studied.

In addition, Fig. 6 validates the PFs got by IHCSA in various K_{max} when the population scale is 100.

Fig. 6 reveals that when K_{max} is set as 100, IHCSA obtains the worst PFs. Meanwhile, it gets the better PFs when the maximum number of iterations is 200. Fig. 6 also verifies the uniform distribution of PFs obtained by iterating 300, 400, and 500 with similar efficiency. Therefore, we choose the maximum number of iterations K_{max} of 300 to reduce computational complexity.

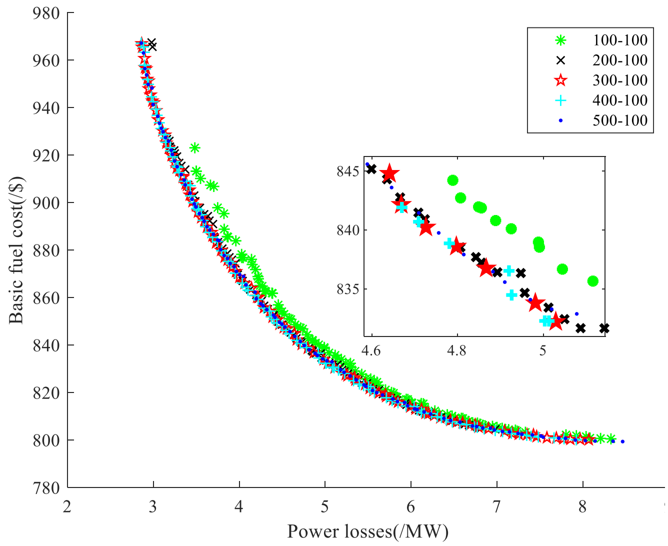

Fig. 6.PFs in various iterations (*NP* = 100)

C. IEEE 30

1) Case1

In Case1, the S_{fcost} and S_{Ploss}, which have a competitive relationship, are optimized by proposed IHCSA, CSA, MOPSO, and NSGA-II approaches in the IEEE30-bus system.

Obviously, The PFs got by the above four methods have been depicted in Fig. 7. Moreover, the results denote that the particle filter performance obtained by IHCSA is significantly better than the ones obtained by MOPSO and NSGA-II. In addition, we are clearly informed that the performance of IHCSA is overwhelmingly superior to that of CSA, which shows that the improved method in this paper has a pronounced effect. It reveals that the proposed IHCSA has excellent potential to realize well-distributed PFs.

TABLE IV depicts the 24-dimensional control variables obtained by the four algorithms, and the BMS received according to the equation (28). Among them, the BMS obtained by the IHCSA algorithm of S_{fcost} and S_{Ploss} are 833.4864 $/h and 4.9817 MW. The ones gained by MOPSO, CSA, and NSGA-II methods, does not perform as well as the former. *CS* depicts control solution.

For Case1, the comparison of BMS derived by different ways is depicted in TABLE V.

2) Case2

In Case2, the S_{fcost} and $S_{emission}$, two important but weakly correlated quantities, need to be optimized concurrently.

Unsurprisingly, Fig. 8 represents PFs achieved by IHCSA, CSA, MOPSO, and NSGA-II methods.

TABLE VI reveals that the BMS obtained by IHCSA has advantages over the ones of the other algorithms. The BMS of the S_{fcost} and $S_{emission}$ are 831.2109 $/h and 0.2469 ton/h. Fig. 8 depicts the Pareto front derived by applying various methods.

TABLE IV
DETAILS OF BMS FOR CASE1

CS	IHCSA	CSA	NSGA-II	MOPSO
P_{Gen_2}(MW)	53.7880	49.9306	56.9084	43.9687
P_{Gen_5}	32.6786	33.6793	32.4266	31.3862
P_{Gen_8}	35.0000	34.8733	33.9626	35.0000
P_{Gen_11}	28.0230	26.4683	26.4354	30.0000
P_{Gen_13}	20.7484	23.4341	21.4147	25.3434
V_{Gen_1}(p.u.)	1.1000	1.0999	1.1000	1.0997
V_{Gen_2}	1.0878	1.0895	1.0898	1.0921
V_{Gen_5}	1.0617	1.0739	1.0652	1.0658
V_{Gen_8}	1.0733	1.0774	1.0715	1.0764
V_{Gen_11}	1.0999	1.0821	1.0273	1.0700
V_{Gen_13}	1.0980	1.0933	1.0438	1.0960
T_{11}(p.u.)	0.9999	1.0937	1.0536	1.1000
T_{12}	0.9479	0.9049	0.9465	0.9000
T_{15}	0.9907	1.0247	1.0629	1.0432
T_{36}	0.9692	1.0153	1.0198	1.0109
Q_{C_10}	0.0334	0.0060	0.0170	0.0500
Q_{C_12}	0.0459	0.0480	0.0261	0.0208
Q_{C_15}	0.0337	0.0489	0.0016	0.0401
Q_{C_17}	0.0500	0.0456	0.0182	0.0475
Q_{C_20}	0.0419	0.0001	0.0431	0.0368
Q_{C_21}	0.0500	0.0415	0.0280	0.0404
Q_{C_23}	0.0381	0.0450	0.0302	0.0113
Q_{C_24}	0.0445	0.0484	0.0451	0.0170
Q_{C_29}	0.0235	0.0365	0.0148	0.0402
S_{Ploss} (MW)	**4.9817**	5.0586	5.2265	5.1268
S_{fcost}($/h)	**833.4864**	834.2233	833.6061	834.5184

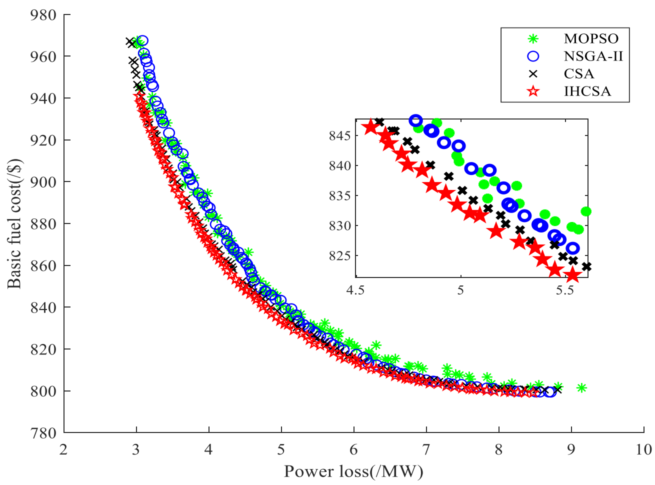

Fig. 7.PFs of Case1

The BMS of Case2 derived by various ways denoted by other academicians in recent years are depicted in TABLE VII.

From the details of TABLE VII, The BMS derived by IHCSA is superior to the ones obtained by NSGA-III, ESDE, and AGSO and has the same competitive advantage as the BMS derived by DE-PFA, MOEA/D, MODFA, and MGBICA. In conclusion, compared with other algorithms proposed by other scholars, the proposed algorithm has better competitive advantages.

TABLE V
VARIOUS BMS FOR CASE1

Comparison	S_{fcost} ($/h)	S_{Ploss} (/MW)
IHCSA	**833.4864**	**4.9817**
CSA	834.2233	5.0586
NSGA-II	833.6061	5.2265
MOPSO	834.5184	5.1268
NSGA-III[27]	836.8076	5.1775
MODFA[27]	833.9365	4.9561

TABLE VI
DETAILS OF BMS FOR CASE2

CS	IHCSA	CSA	NSGA-II	MOPSO
P_{Gen_2}(MW)	57.9900	58.9863	58.9102	59.8005
P_{Gen_5}	25.6644	26.5294	28.2860	25.0199
P_{Gen_8}	35.0000	34.9108	34.9837	33.0113
P_{Gen_11}	27.0888	27.1162	25.4120	23.5310
P_{Gen_13}	26.2415	24.7357	24.4445	29.5362
V_{Gen_1}(p.u.)	1.1000	1.0967	1.0589	1.1000
V_{Gen_2}	1.0876	1.0870	1.0467	1.0916
V_{Gen_5}	1.0666	1.0525	1.0117	1.0486
V_{Gen_8}	1.0676	1.0635	1.0249	1.0790
V_{Gen_11}	1.0973	0.9844	1.0810	1.0896
V_{Gen_13}	1.0766	1.0590	1.0567	1.0807
T_{11}(p.u.)	1.0410	1.0662	0.9083	0.9978
T_{12}	0.9447	0.9500	1.0466	0.9875
T_{15}	1.0090	1.0939	0.9972	1.1000
T_{36}	0.9888	1.0371	0.9757	1.0280
Q_{C_10}	0.0368	0.0414	0.0347	0.0240
Q_{C_12}	0.0500	0.0016	0.0471	0.0500
Q_{C_15}	0.0438	0.0115	0.0018	0.0320
Q_{C_17}	0.0358	0.0297	0.0114	0.0500
Q_{C_20}	0.0500	0.0180	0.0056	0.0294
Q_{C_21}	0.0416	0.0001	0.0408	0.0490
Q_{C_23}	0.0221	0.0498	0.0478	0.0066
Q_{C_24}	0.0500	0.0179	0.0356	0.0300
Q_{C_29}	0.0308	0.0498	0.0334	0.0349
$S_{emission}$(MW)	**0.2469**	0.2472	0.2478	0.2492
S_{fcost}($/h)	**831.2109**	831.9036	832.3313	831.3669

TABLE VII
VARIOUS BMS FOR CASE2

Comparison	S_{fcost} (/$)	$S_{emission}$ (ton/h)
IHCSA	**831.2109**	**0.2464**
CSA	831.9036	0.2472
NSGA-II	832.3313	0.2478
MOPSO	831.3669	0.2492
NSGA-III[27]	832.5323	0.2483
DE-PFA[28]	833.5200	0.2332

3) Case3

In Case3, IHCSA and the other three algorithms are applied to optimize S_{Ploss} and S_{fcost_vp} simultaneously. As shown in TABLE VIII, the BMS obtained by the IHCSA algorithm has advantages over the other three algorithms, including S_{fcost_vp} of 864.7519 $/h and S_{Ploss} of 5.5995 MW. Fig. 9 reveals the Pareto front of POS obtained by the

IHCSA algorithm is more prominent, indicating that the effect of the proposed method is remarkable.

TABLE IX denotes that compared with the algorithms proposed by other scholars, the BMS obtained by IHCSA has more advantages.

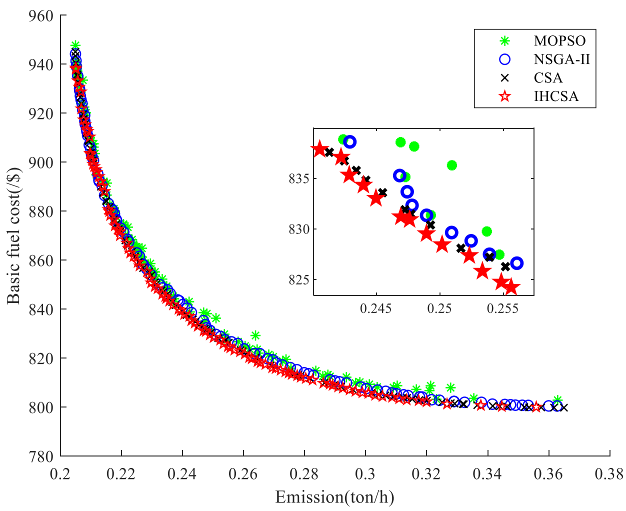

Fig. 8.PFs of Case2

TABLE VIII
DETAILS OF BMS FOR CASE3

CS	IHCSA	CSA	NSGA-II	MOPSO
P_{Gen_2}(MW)	44.5546	46.4769	44.7199	40.0518
P_{Gen_5}	30.7240	33.9651	29.7495	30.0146
P_{Gen_8}	34.8646	34.8515	34.9995	35.0000
P_{Gen_11}	28.0515	19.2982	27.0462	30.0000
P_{Gen_13}	15.8929	19.7758	18.7778	17.3900
V_{Gen_1}(p.u.)	1.1000	1.0994	1.0962	1.1000
V_{Gen_2}	1.0862	1.0886	1.0821	1.0850
V_{Gen_5}	1.0634	1.0676	1.0552	1.0591
V_{Gen_8}	1.0706	1.0712	1.0679	1.0677
V_{Gen_11}	1.1000	1.0666	1.0717	1.0925
V_{Gen_13}	1.0997	1.0839	1.0973	1.0845
T_{11}(p.u.)	1.0149	1.0287	0.9821	1.0636
T_{12}	0.9344	0.9559	0.9503	0.9000
T_{15}	0.9896	1.0013	0.9953	1.0032
T_{36}	0.9685	0.9912	0.9848	0.9825
Q_{C_10}	0.0481	0.0092	0.0500	0.0192
Q_{C_12}	0.0500	0.0158	0.0372	0.0136
Q_{C_15}	0.0345	0.0020	0.0260	0.0373
Q_{C_17}	0.0500	0.0105	0.0167	0.0284
Q_{C_20}	0.0348	0.0456	0.0432	0.0500
Q_{C_21}	0.0500	0.0449	0.0380	0.0500
Q_{C_23}	0.0390	0.0281	0.0159	0.0430
Q_{C_24}	0.0500	0.0290	0.0466	0.0500
Q_{C_29}	0.0290	0.0347	0.0242	0.0337
S_{Ploss} (MW)	**5.5995**	5.7337	5.6830	5.6490
$S_{fcost\text{-}vp}$($/h)	**864.7519**	865.7643	866.0764	867.3759

4) Case4

In Case4, two objectives are considered and optimized concurrently by various methods, including basic fuel cost and voltage deviation. TABLE X indicates that the BMS obtained by the IHCSA algorithm includes a voltage deviation of 0.4366 and basic fuel cost of 799.6643 $/h.

As can be seen from Fig. 10, the Pareto frontier of IHCSA has more advantages than CSA and NSGA-II. The Pareto frontier of the MOPSO algorithm is not ideal, so no comparison is made.

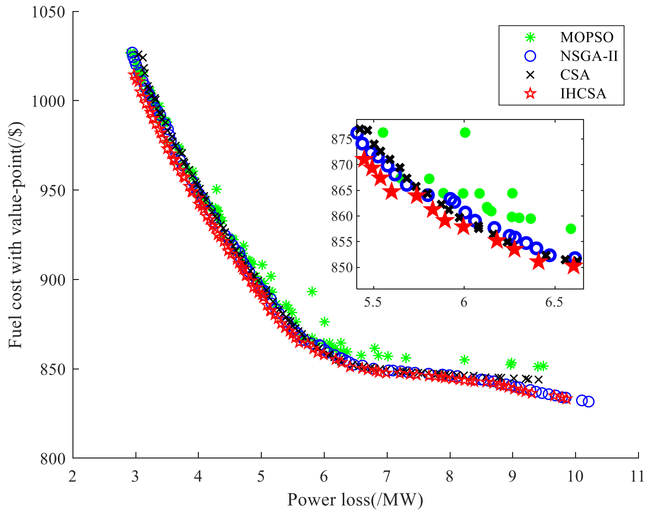

Fig. 9.PFs of Case3

TABLE IX
VARIOUS BMS FOR CASE3

Comparison	S_{fcost_vp} ($/h)	S_{Ploss} (/MW)
IHCSA	**864.7519**	**5.5995**
CSA	865.7643	5.7337
NSGA-II	866.0764	5.6830
MOPSO	867.3759	5.6490
MHFPA[40]	867.8159	5.6303
NHBA[28]	868.9526	5.6761

TABLE X
DETAILS OF BMS FOR CASE4

CS	IHCSA	CSA	NSGA-II
P_{Gen_2}(MW)	49.6677	49.6029	48.9956
P_{Gen_5}	21.1507	21.8197	21.2636
P_{Gen_8}	21.3810	20.4622	21.3171
P_{Gen_11}	11.7276	13.4931	10.6560
P_{Gen_13}	12.0223	12.2405	12.0521
V_{Gen_1}(p.u.)	1.1000	1.0542	1.0995
V_{Gen_2}	1.0869	1.0342	1.0837
V_{Gen_5}	1.0529	0.9987	1.0532
V_{Gen_8}	1.0624	0.9992	1.0618
V_{Gen_11}	1.0335	1.0144	1.0454
V_{Gen_13}	1.0338	1.0309	1.0494
T_{11}(p.u.)	1.0485	0.9365	1.0159
T_{12}	1.0331	0.9597	1.0765
T_{15}	1.0713	0.9717	1.0799
T_{36}	1.0094	0.9440	1.0273
Q_{C_10}	0.0414	0.0230	0.0495
Q_{C_12}	0.0000	0.0361	0.0358
Q_{C_15}	0.0461	0.0142	0.0095
Q_{C_17}	0.0292	0.0294	0.0414
Q_{C_20}	0.0500	0.0131	0.0220
Q_{C_21}	0.0358	0.0249	0.0279
Q_{C_23}	0.0287	0.0233	0.0244
Q_{C_24}	0.0500	0.0296	0.0500
Q_{C_29}	0.0182	0.0109	0.0258
S_{VD}	**0.4366**	0.2132	0.4681
S_{fcost} ($/h)	**799.6643**	803.2034	799.6652

5) Case5

In Case5, the S_{fcost}, $S_{emission}$, and S_{Ploss} are optimized concurrently. TABLE XI reveals that the BMS obtained by IHCSA has more advantages, including $S_{emission}$ of 0.2177 ton/h, S_{Ploss} of 4.0638 MW, and S_{fcost} of 876.2110 $/h.

For Case5, the comparison of the BMS obtained by different algorithms is denoted in TABLE XIII.

Fig. 11 shows that Pareto front of IHCSA is nearer actual Pareto front than CSA, NSGA-II, and MOPSO.

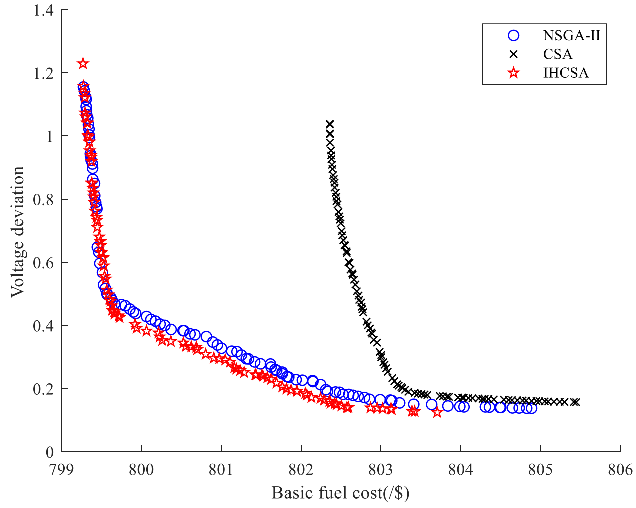

Fig. 10. PFs of Case4

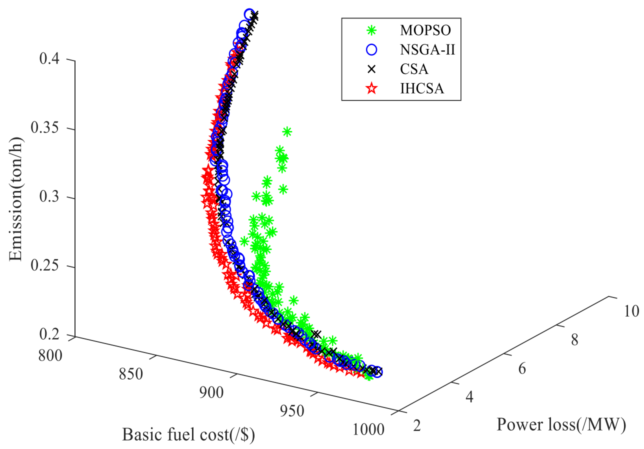

Fig. 11. PFs of Case5

TABLE XI
DETAILS OF BMS FOR CASE5

CS	IHCSA	CSA	NSGA-II	MOPSO
P_{Gen_2}(MW)	59.2651	66.5689	62.5712	80.000
P_{Gen_5}	37.4872	38.2036	41.5270	33.8435
P_{Gen_8}	35.0000	34.0128	34.7084	35.0000
P_{Gen_11}	30.0000	28.7128	28.3620	27.3982
P_{Gen_13}	35.6421	32.8182	32.1899	32.1505
V_{Gen_1}(p.u.)	1.1000	1.0811	1.0508	1.1000
V_{Gen_2}	1.0871	1.07017	1.0443	1.1000
V_{Gen_5}	1.0641	1.0412	1.0209	1.0795
V_{Gen_8}	1.0739	1.0380	1.0260	1.0787
V_{Gen_11}	1.0777	1.0686	1.0614	1.1000
V_{Gen_13}	1.0656	1.0851	1.0682	1.0895
T_{11}(p.u.)	1.0072	0.9135	0.9409	0.9801
T_{12}	1.0287	0.9563	1.0053	1.0670
T_{15}	1.0489	0.9491	1.0269	0.9774
T_{36}	1.0215	0.9463	0.9666	0.9599
Q_{C_10}	0.0149	0.0139	0.0178	0.0500
Q_{C_12}	0.0283	0.0041	0.0287	0.0004
Q_{C_15}	0.0454	0.0427	0.0325	0.0158
Q_{C_17}	0.0444	0.0488	0.0144	0.0323
Q_{C_20}	0.0500	0.0472	0.0215	0.0454
Q_{C_21}	0.0127	0.0161	0.0471	0.0447
Q_{C_23}	0.0327	0.0125	0.0014	0.0321
Q_{C_24}	0.0274	0.0136	0.0367	0.0406
Q_{C_29}	0.0255	0.0300	0.0420	0.0283
$S_{emission}$(ton/h)	**0.2177**	0.2184	0.2177	0.2203
S_{Ploss} (MW)	**4.0638**	4.3548	4.2449	4.1235
S_{fcost}($/h)	**876.2110**	879.3365	883.6450	886.3948

6) Case6

In Case6, the power loss and emission are chosen to be optimized simultaneously. The BMS obtained by four algorithms, including IHCSA, CSA, NSGA-II, and MOPSO, are shown in TABLE XII.

It is apparent from the table the BMS gained by IHCSA of the emission and the active power loss is 0.2053 ton/h and 2.8929 MW. The Pareto front of their POS is indicated in Fig. 12. It is evident that the Pareto front of the IHCSA algorithm has outstanding advantages.

TABLE XIV indicates that compared to other researches, the BMS obtained by IHCSA has strong competitiveness.

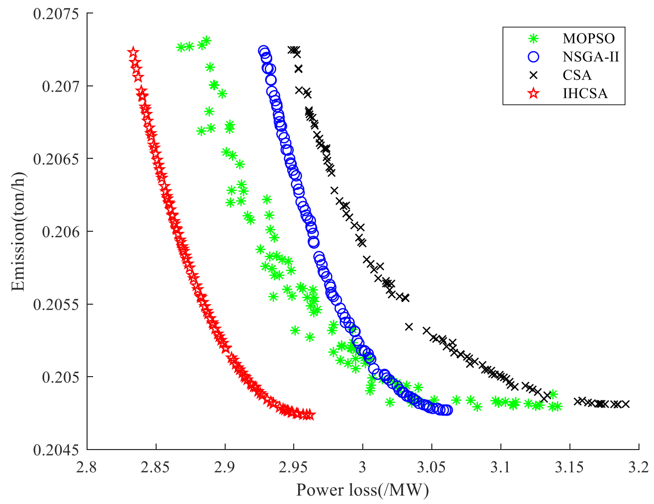

Fig. 12. PFs of Case6

TABLE XII
DETAILS OF BMS FOR CASE6

CS	IHCSA	CSA	NSGA-II	MOPSO
P_{Gen_2}(MW)	73.5921	73.4866	73.7064	73.1661
P_{Gen_5}	50.0000	49.9996	49.9992	49.9271
P_{Gen_8}	34.9999	34.9917	34.9999	34.9268
P_{Gen_11}	30.0000	29.9992	29.9987	29.9741
P_{Gen_13}	40.0000	39.9979	39.9992	39.9879
V_{Gen_1}(p.u.)	1.1000	1.1000	1.0759	1.0999
V_{Gen_2}	1.0964	1.1000	1.0712	1.0984
V_{Gen_5}	1.07841	1.0863	1.0530	1.0801
V_{Gen_8}	1.0856	1.0986	1.0589	1.0854
V_{Gen_11}	1.1000	1.0817	1.0980	1.1000
V_{Gen_13}	1.1000	1.1000	1.0998	1.0940
T_{11}(p.u.)	1.0208	0.9614	1.0115	1.0144
T_{12}	0.9287	1.0772	0.9000	0.9860
T_{15}	0.9867	1.0055	0.9646	0.9855
T_{36}	0.9706	1.0186	0.9523	0.9999
Q_{C_10}	0.0211	0.0500	0.0479	0.0480
Q_{C_12}	0.0500	0.0005	0.0479	0.0000
Q_{C_15}	0.0401	0.0000	0.0500	0.0455
Q_{C_17}	0.0500	0.0000	0.0469	0.0500
Q_{C_20}	0.0441	0.0375	0.0288	0.0306
Q_{C_21}	0.0500	0.0419	0.0479	0.0500
Q_{C_23}	0.0292	0.0500	0.0317	0.0142
Q_{C_24}	0.0500	0.0462	0.0483	0.0419
Q_{C_29}	0.0203	0.0469	0.0229	0.0398
$S_{emission}$(ton/h)	**0.2053**	0.2053	0.2053	0.2053
S_{Ploss} (MW)	**2.8929**	3.0333	2.9872	2.9508

TABLE XIII
VARIOUS BMS FOR CASE5

Comparison	$S_{emission}$ (ton/h)	S_{Ploss} (/MW)	S_{fcost} ($/h)
IHCSA	**0.2177**	**4.0638**	**876.2110**
CSA	0.2184	4.3548	879.3365
NSGA-II	0.2177	4.2449	883.6450
MOPSO	0.2203	4.1235	886.3948
MHFPA[40]	0.2167	3.9070	879.4391

TABLE XIV
VARIOUS BMS FOR CASE6

Comparison	$S_{emission}$ (ton/h)	S_{Ploss} (/MW)
IHCSA	**0.2053**	**2.8929**
CSA	0.2053	3.0333
NSGA-II	0.2053	2.9872
MOPSO	0.2053	2.9508
MODFA[27]	0.2054	2.8830

TABLE XV
DETAILS OF BMS FOR CASE7

CS	IHCSA	CSA	NSGA-II
P_{Gen_2}(MW)	72.9442	99.9283	71.3663
P_{Gen_3}	57.4972	66.5498	55.8950
P_{Gen_6}	90.7924	76.8989	85.5446
P_{Gen_8}	378.3653	372.3670	392.4783
P_{Gen_9}	100.0000	100.0000	100.0000
P_{Gen_12}	410.0000	410.0000	408.5869
V_{Gen_1}(p.u.)	1.0568	1.0872	0.9863
V_{Gen_2}	1.0533	1.0867	0.9834
V_{Gen_3}	1.0467	1.0833	0.9815
V_{Gen_6}	1.0513	1.0810	1.0007
V_{Gen_8}	1.0545	1.0818	1.0089
V_{Gen_9}	1.0473	1.0779	0.9983
V_{Gen_12}	1.0453	1.0751	0.9844
T_{19}(p.u.)	1.0130	0.9160	0.9776
T_{20}	0.9117	1.0354	1.0287
T_{31}	0.9796	1.0996	1.0084
T_{35}	0.9988	1.0177	1.0080
T_{36}	1.0123	1.0769	1.0162
T_{37}	1.0362	1.0291	0.9463
T_{41}	0.9952	1.0232	0.9108
T_{46}	0.9587	0.9729	0.9464
T_{54}	0.9012	0.9659	0.9023
T_{58}	0.9611	0.9995	0.9244
T_{59}	0.9570	1.0184	0.9262
T_{65}	0.9944	1.0030	0.9361
T_{66}	0.9311	0.9711	0.9076
T_{71}	0.9476	0.9877	0.9574
T_{73}	0.9727	0.9576	1.0041
T_{76}	0.9514	1.0365	0.9237
T_{80}	1.0144	1.0207	0.9360
$Qc_{\_18}$(p.u.)	0.1002	0.0966	0.1895
$Qc_{\_25}$	0.1522	0.1446	0.2089
$Qc_{\_53}$	0.1372	0.1870	0.1488
S_{Ploss} (MW)	**11.3468**	11.4242	12.7539
S_{fcost}($/h)	**41989.0500**	42096.1600	41961.0000

D. IEEE 57

1) Case7

In Case7, the S_{fcost} and S_{Ploss} are still treated as two weakly correlated targets for optimization, however, the platform for testing is changed to the IEEE57-bus system.

In this case, since the POS of the MOPSO algorithm cannot obtain an effective Pareto front, its analysis is not carried out. The BMS of IHCSA, CSA, and NSGA-II are depicted in TABLE XV.

As shown in the table, the one gained by proposed approach includes S_{Ploss} of 11.3468 MW and S_{fcost} of 41989.0500 $/h.

It is apparent from Fig. 13 that the Pareto front of the POS obtained by IHCSA has a greater tendency to be appreciated by managers. There is no doubt that compared with the other two algorithms, IHCSA has more advantages.

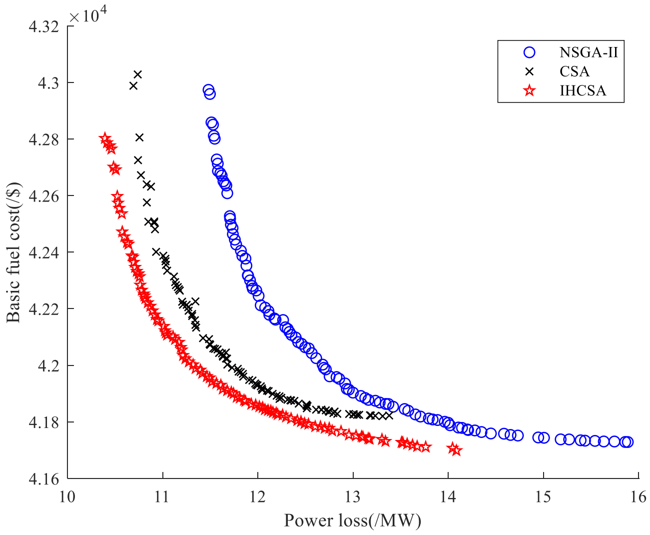

Fig. 13. PFs of Case7

TABLE XVI
VARIOUS BMS FOR CASE7

Algorithms	S_{fcost} ($/h)	S_{Ploss} (/MW)
IHCSA	**41989.0500**	**11.3468**
CSA	42096.1600	11.4242
NSGA-II	41961.0000	12.7539
ESDE-MC[24]	41998.3588	11.8415

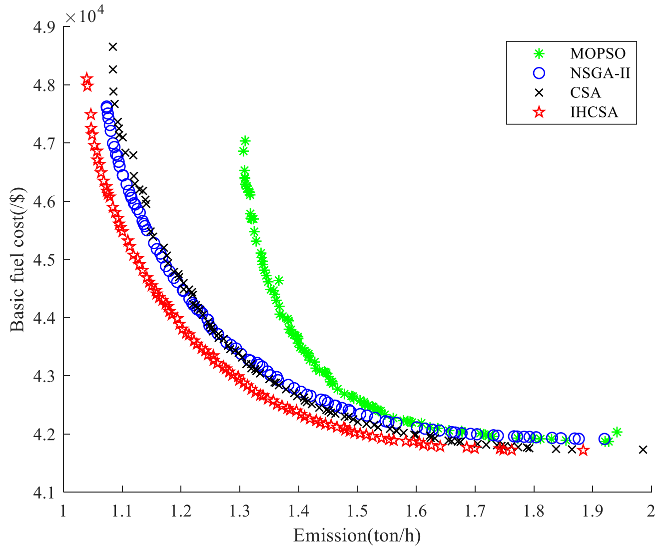

Fig. 14. PFs of Case8

TABLE XVII
VARIOUS BMS FOR CASE8

Comparison	S_{fcost} ($/h)	$S_{emission}$ (ton/h)
IHCSA	**42923.5900**	**1.2989**
CSA	43125.2700	1.3194
NSGA-II	43007.9400	1.3518
MOPSO	43056.2700	1.3100
MODFA[27]	43174.5700	1.2679
NSGA-III[27]	43398.7500	1.2530

TABLE XVIII
VARIOUS BMS FOR CASE9

Algorithms	S_{fcost} (\$/h)	S_{Ploss} (/MW)
IHCSA	**58513.8900**	**54.3803**
NSGA-II	59366.9100	56.8467
HFBA-COFS[28]	59624.0613	61.0362

2) Case8

In Case8, the S_{fcost} and $S_{emission}$ are synchronously optimized by four algorithms to reflect the distinctions between the different methods. As shown in Fig. 14, compared with CSA, NSGA-II and MOPSO, the Pareto front gained by IHCSA is nearer to the real Pareto front and has more advantages. The BMS and corresponding variables obtained are depicted in TABLE XIX, including emission of 1.2989 ton/h and fuel cost of 42923.5900 \$/h.

TABLE XIX
DETAILS OF BMS FOR CASE8

CS	IHCSA	CSA	NSGA-II	MOPSO
P_{Gen_2}(MW)	100.0000	93.1424	99.8112	100.0000
P_{Gen_3}	81.9845	87.7182	76.7071	100.9952
P_{Gen_6}	100.0000	98.8348	100.0000	97.7089
P_{Gen_8}	334.9970	342.1080	350.3993	360.8372
P_{Gen_9}	100.0000	92.0777	99.9511	100.0000
P_{Gen_12}	332.6469	329.4928	332.6281	313.0755
V_{Gen_1}(p.u.)	1.0481	1.0985	0.9421	1.1000
V_{Gen_2}	1.0460	1.0965	0.9376	1.1000
V_{Gen_3}	1.0407	1.0907	0.9566	1.1000
V_{Gen_6}	1.0428	1.0863	0.9965	1.1000
V_{Gen_8}	1.0512	1.0827	1.0301	1.1000
V_{Gen_9}	1.0408	1.0694	1.0119	1.1000
V_{Gen_12}	1.0274	1.0679	1.0079	1.1000
T_{19}(p.u.)	1.0173	0.9458	1.0054	0.9197
T_{20}	0.9349	1.0988	1.0120	1.0745
T_{31}	1.0043	1.0883	0.9077	1.1000
T_{35}	0.9982	0.9974	0.9400	1.1000
T_{36}	0.9640	0.9214	1.0998	1.0426
T_{37}	1.0320	1.0884	1.0304	1.0781
T_{41}	0.9837	0.9846	0.9776	1.0346
T_{46}	0.9326	0.9007	1.0244	0.9352
T_{54}	0.9251	0.9059	0.9074	0.9309
T_{58}	0.9590	0.9757	0.9011	1.0242
T_{59}	0.9472	1.0068	0.9146	1.0046
T_{65}	0.9559	1.0316	0.9839	1.0482
T_{66}	0.9287	0.9402	0.9999	0.9860
T_{71}	0.9529	1.0865	1.0081	0.9888
T_{73}	1.0137	0.9013	1.0093	0.9861
T_{76}	0.9670	1.0148	0.9567	0.9874
T_{80}	0.9936	1.0337	0.9812	1.0950
Q_{C_18}(p.u.)	0.0575	0.2035	0.1329	0.0135
Q_{C_25}	0.1290	0.0025	0.2648	0.1894
Q_{C_53}	0.1266	0.0240	0.1667	0.2987
$S_{emission}$(ton/h)	**1.2989**	1.3194	1.3518	1.3100
S_{fcost}(\$/h)	**42923.5900**	43125.2700	43007.9400	43056.2700

TABLE XVII reveals that compared with other scholars' methods, the BMS obtained by IHCSA has a more significant advantage in basic fuel cost. Meanwhile, IHCSA can also achieve good results in optimizing emissions.

E. IEEE 118

Due to the uniqueness and complex structure of the IEEE 118-bus system, few scholars have studied the adaptability of their methods above. Because the work is quite difficult.

1) Case9

In Case9, the S_{fcost} and S_{Ploss} will be calculated in the IEEE118-bus system which is more challenging.

Owing to the Pareto frontier derived by CSA and MOPSO methods in the IEEE118-bus system is uneven and has a strong discrete type, which are not compared in this part. The delightful thing is that the PF of IHCSA is well-distributed from Fig. 15, and its distribution has more significant advantages.

The BMS obtained by IHCSA, including active power loss of 54.3803MW and basic fuel cost of 58513.8900 \$/h, has obvious benefits over NSGA-II. TABLE XX reveals detailed comparison data.

TABLE XVIII depicts that the BMS gained by the proposed IHCSA approach has significant advantages.

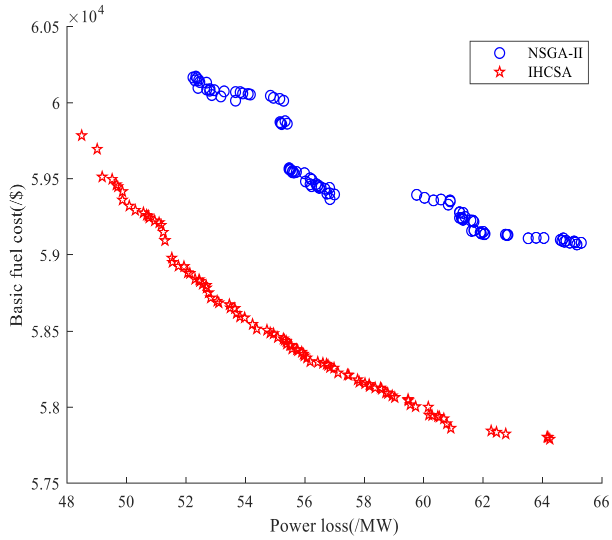

Fig. 15. PFs of Case9

2) Case10

In Case10, the S_{fcost} and $S_{emission}$ are synchronously optimized by the proposed IHCSA and NSGA-II approaches to reflect the distinctions between the different methods.

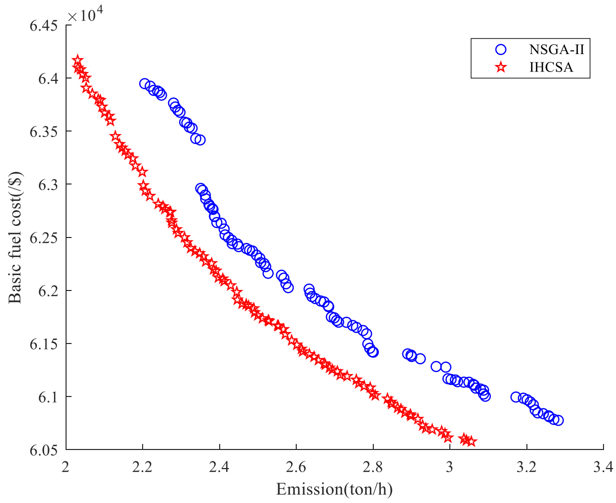

Fig. 16. PFs of Case10

This case can thoroughly test the optimization ability of the above two methods in a large test system. To provide decision-makers with a practical reference value of an excellent control scheme.

Fig. 16 depicts that the PF of IHCSA is nearer to the real PF. Compared with NSGA-II, its distribution has significant advantages. The BMS obtained by IHCSA, including emission of 2.4463 ton/h and basic fuel cost of 61912.0100 \$/h, has obvious advantages over NSGA-II in TABLE XXI.

VI. Performance Evaluation

In this paper, the PFs obtained by different algorithms are quantitatively analyzed by SP and HV. Meanwhile, eight optimization cases on IEEE30- and IEEE57-bus systems are taken as experimental objects for comprehensive analysis and research. The optimization performance of IHCSA, CSA, NSGA-II, and MOPSO algorithms are compared.

TABLE XX
DETAILS OF BMS FOR CASE9

CS	IHCSA	NSGA-II	*CS*	IHCSA	NSGA-II
P_{Gen_4}(MW)	5.0070	5.2445	V_{Gen_26}	0.9979	1.0057
P_{Gen_6}	5.0000	11.6364	V_{Gen_27}	0.9975	1.0091
P_{Gen_8}	5.0000	12.3650	V_{Gen_31}	1.0018	1.0109
P_{Gen_10}	202.9974	179.6695	V_{Gen_32}	1.0295	0.9928
P_{Gen_12}	244.3541	230.5180	V_{Gen_34}	1.0333	0.9977
P_{Gen_15}	18.4481	14.8453	V_{Gen_36}	1.0247	0.9686
P_{Gen_18}	68.6539	25.4540	V_{Gen_40}	1.0212	0.9535
P_{Gen_19}	15.1861	19.2120	V_{Gen_42}	1.0006	1.0417
P_{Gen_24}	5.7228	11.6513	V_{Gen_46}	1.0291	1.0405
P_{Gen_25}	100.6194	141.3584	V_{Gen_49}	1.0393	1.0462
P_{Gen_26}	277.6701	282.6833	V_{Gen_54}	1.0409	1.0527
P_{Gen_27}	8.0192	22.8670	V_{Gen_55}	1.0385	1.0489
P_{Gen_31}	8.0000	8.1908	V_{Gen_56}	1.0315	1.0558
P_{Gen_32}	64.7472	29.3844	V_{Gen_59}	1.0230	1.0369
P_{Gen_34}	8.9427	15.7024	V_{Gen_61}	1.0210	1.0182
P_{Gen_36}	53.9848	30.9166	V_{Gen_62}	1.0240	1.0205
P_{Gen_40}	8.0000	8.2890	V_{Gen_65}	1.0336	1.0478
P_{Gen_42}	8.3483	17.4059	V_{Gen_66}	1.0352	1.0397
P_{Gen_46}	29.6067	26.2924	V_{Gen_69}	1.0103	1.0260
P_{Gen_49}	250.0000	162.6309	V_{Gen_70}	0.9936	0.9970
P_{Gen_54}	185.6555	186.7033	V_{Gen_72}	1.0165	1.0681
P_{Gen_55}	64.5565	60.8435	V_{Gen_73}	1.0008	0.9882
P_{Gen_56}	42.9506	43.9825	V_{Gen_74}	1.0099	1.0292
P_{Gen_59}	87.6784	148.8000	V_{Gen_76}	1.0201	1.0311
P_{Gen_61}	107.8828	110.3558	V_{Gen_77}	1.0259	1.0377
P_{Gen_62}	25.0254	74.1492	V_{Gen_80}	1.0023	1.0280
P_{Gen_65}	287.1492	248.7397	V_{Gen_85}	0.9845	0.9823
P_{Gen_66}	266.7079	343.5521	V_{Gen_87}	0.9734	0.9299
P_{Gen_69}	37.0283	50.4957	V_{Gen_89}	1.0089	1.0110
P_{Gen_70}	10.0464	12.1782	V_{Gen_90}	1.0120	1.0002
P_{Gen_72}	6.1457	6.7566	V_{Gen_91}	1.0195	0.9886
P_{Gen_73}	5.3039	11.9832	V_{Gen_92}	1.0088	1.0106
P_{Gen_74}	77.0225	54.9103	V_{Gen_99}	1.0291	0.9992
P_{Gen_76}	25.0000	30.2879	V_{Gen_100}	1.0033	1.0103
P_{Gen_77}	189.3974	175.5451	V_{Gen_103}	0.9760	1.0086
P_{Gen_80}	28.3737	84.6949	V_{Gen_104}	0.9923	1.0307
P_{Gen_85}	10.0000	11.1145	V_{Gen_105}	0.9992	1.0240
P_{Gen_87}	142.1183	100.1340	V_{Gen_107}	0.9811	0.9848
P_{Gen_89}	50.9175	91.6709	V_{Gen_110}	1.0326	0.9847
P_{Gen_90}	8.0047	8.0766	V_{Gen_111}	1.0343	1.0406
P_{Gen_91}	20.6452	36.8795	V_{Gen_112}	1.0384	0.9920
P_{Gen_92}	105.3042	103.4046	V_{Gen_113}	1.0173	1.0376
P_{Gen_99}	100.0000	100.3301	V_{Gen_116}	1.0279	1.0256
P_{Gen_100}	144.3055	100.0000	T_8(p.u.)	0.9566	0.9125
P_{Gen_103}	13.3264	16.7799	T_{32}	0.9424	1.0959
P_{Gen_104}	25.4175	33.9713	T_{36}	0.9742	0.9269
P_{Gen_105}	64.4166	30.5079	T_{51}	0.9757	0.9966
P_{Gen_107}	13.5434	8.0083	T_{93}	0.9729	1.0445
P_{Gen_110}	34.1036	31.5933	T_{95}	0.9922	0.9467
P_{Gen_111}	25.0000	25.6738	T_{102}	0.9810	1.0700
P_{Gen_112}	25.2142	25.0562	T_{107}	1.0204	1.0832
P_{Gen_113}	28.0893	30.5120	T_{127}	1.0153	0.9838
P_{Gen_116}	45.2644	29.2948	Q_{C_34}(p.u.)	0.0135	0.2515
V_{Gen_1}(p.u.)	0.9982	1.0612	Q_{C_44}	0.2674	0.1726
V_{Gen_4}	0.9995	1.0571	Q_{C_45}	0.1380	0.1936
V_{Gen_6}	0.9932	0.9714	Q_{C_46}	0.1797	0.1473
V_{Gen_8}	1.0255	0.9956	Q_{C_48}	0.2402	0.1688
V_{Gen_10}	1.0018	1.0503	Q_{C_74}	0.1897	0.1611
V_{Gen_12}	1.0184	1.0109	Q_{C_79}	0.2443	0.1475
V_{Gen_15}	1.0200	1.0371	Q_{C_82}	0.1783	0.2961
V_{Gen_18}	1.0174	1.0156	Q_{C_83}	0.1182	0.0999
V_{Gen_19}	1.0035	1.0301	Q_{C_105}	0.2050	0.2617
V_{Gen_24}	0.9899	1.0170	Q_{C_107}	0.2013	0.2080
V_{Gen_25}	1.0125	1.0835	Q_{C_110}	0.1381	0.0988
			S_{Ploss} (MW)	**54.3803**	56.8467
			S_{fcost} ($/h)	**58513.8900**	59366.9100

A. SP

The SP decipts the criterion deviation of two neighboring solutions in a set composed of mutually non-dominant solutions[28]. It can be described as (34).

$$SP = \sqrt{\sum_{i=1}^{n}\left(d_{\text{average}} - d_i\right)^2} \tag{34}$$

$$d_i = \min_{o=1,2,\cdots,n}\left(\sum_{m=1}^{M}\left|f_m^i - f_m^o\right|\right) \tag{35}$$

TABLE XXI
DETAILS OF BMS FOR CASE10

CS	IHCSA	NSGA-II	*CS*	IHCSA	NSGA-II
P_{Gen_4}(MW)	5.1230	7.1794	V_{Gen_26}	1.0363	1.0732
P_{Gen_6}	12.8263	10.8971	V_{Gen_27}	0.9749	1.0234
P_{Gen_8}	5.0000	11.1832	V_{Gen_31}	0.9606	1.0040
P_{Gen_10}	193.5924	284.9689	V_{Gen_32}	0.9926	1.0464
P_{Gen_12}	179.7772	201.4346	V_{Gen_34}	0.9938	1.0412
P_{Gen_15}	18.6344	11.9599	V_{Gen_36}	0.9917	0.9990
P_{Gen_18}	45.1393	46.0954	V_{Gen_40}	1.0178	1.0318
P_{Gen_19}	5.0000	16.6181	V_{Gen_42}	1.0264	1.0004
P_{Gen_24}	5.0000	5.4499	V_{Gen_46}	1.0324	1.0218
P_{Gen_25}	100.0000	101.3249	V_{Gen_49}	1.0262	1.0102
P_{Gen_26}	100.0000	121.9729	V_{Gen_54}	1.0316	0.9913
P_{Gen_27}	8.0000	28.6342	V_{Gen_55}	1.0286	1.0085
P_{Gen_31}	8.5877	18.4879	V_{Gen_56}	1.0292	0.9530
P_{Gen_32}	99.3617	42.3373	V_{Gen_59}	0.9924	1.0294
P_{Gen_34}	21.4048	23.9431	V_{Gen_61}	1.0164	1.0315
P_{Gen_36}	25.0000	25.2501	V_{Gen_62}	1.0197	0.9947
P_{Gen_40}	9.9399	15.0700	V_{Gen_65}	1.0365	0.9683
P_{Gen_42}	10.8984	8.0001	V_{Gen_66}	0.9958	1.0880
P_{Gen_46}	95.6233	90.9803	V_{Gen_69}	0.9831	0.9720
P_{Gen_49}	136.3450	247.0106	V_{Gen_70}	0.9703	0.9407
P_{Gen_54}	128.9885	121.6719	V_{Gen_72}	1.0340	1.0447
P_{Gen_55}	38.3923	64.4345	V_{Gen_73}	0.9670	1.0425
P_{Gen_56}	38.0486	30.1118	V_{Gen_74}	1.0018	1.0219
P_{Gen_59}	50.0000	50.8094	V_{Gen_76}	1.0144	1.0239
P_{Gen_61}	188.1862	89.9062	V_{Gen_77}	0.9973	1.0062
P_{Gen_62}	78.8032	46.8959	V_{Gen_80}	1.0081	1.0179
P_{Gen_65}	221.2279	363.5226	V_{Gen_85}	0.9901	1.0352
P_{Gen_66}	213.7170	150.6464	V_{Gen_87}	1.0119	0.9514
P_{Gen_69}	30.6825	30.7475	V_{Gen_89}	1.0308	0.9962
P_{Gen_70}	16.3638	13.6647	V_{Gen_90}	1.0169	1.0456
P_{Gen_72}	22.0174	20.3617	V_{Gen_91}	1.0114	0.9773
P_{Gen_73}	5.0183	20.0000	V_{Gen_92}	1.0436	0.9959
P_{Gen_74}	47.1793	34.1392	V_{Gen_99}	1.0760	0.9765
P_{Gen_76}	51.2797	40.6316	V_{Gen_100}	1.0489	1.0317
P_{Gen_77}	300.0000	164.8704	V_{Gen_103}	1.0226	0.9530
P_{Gen_80}	62.5641	32.9637	V_{Gen_104}	1.0108	0.9456
P_{Gen_85}	16.8765	23.5636	V_{Gen_105}	1.0616	0.9694
P_{Gen_87}	207.2688	208.6281	V_{Gen_107}	1.0175	0.9307
P_{Gen_89}	60.5256	72.2084	V_{Gen_110}	1.0148	1.0016
P_{Gen_90}	12.0636	10.3985	V_{Gen_111}	1.0012	0.9786
P_{Gen_91}	20.3372	24.7075	V_{Gen_112}	0.9766	1.0385
P_{Gen_92}	212.9350	142.1519	V_{Gen_113}	1.0301	1.0022
P_{Gen_99}	201.4881	183.9215	V_{Gen_116}	0.9919	0.9728
P_{Gen_100}	201.7482	250.0860	T_8(p.u.)	0.9677	1.0707
P_{Gen_103}	13.0096	8.4881	T_{32}	0.9000	0.9692
P_{Gen_104}	25.1885	25.2804	T_{36}	0.9675	0.9718
P_{Gen_105}	25.0000	25.9516	T_{51}	1.0177	0.9118
P_{Gen_107}	8.2824	13.4831	T_{93}	0.9720	1.0869
P_{Gen_110}	35.0056	33.9498	T_{95}	1.0251	0.9338
P_{Gen_111}	27.8755	30.7207	T_{102}	1.0396	0.9776
P_{Gen_112}	47.9383	31.4164	T_{107}	0.9866	0.9769
P_{Gen_113}	51.3876	43.5494	T_{127}	0.9871	0.9955
P_{Gen_116}	36.9834	35.8061	Q_{C_34}(p.u.)	0.1356	0.2750
V_{Gen_1}(p.u.)	1.0270	1.0154	Q_{C_44}	0.1989	0.2258
V_{Gen_4}	1.0433	0.9871	Q_{C_45}	0.2651	0.0165
V_{Gen_6}	0.9770	1.0575	Q_{C_46}	0.0577	0.2895
V_{Gen_8}	0.9769	1.0783	Q_{C_48}	0.1747	0.1436
V_{Gen_10}	0.9798	0.9818	Q_{C_74}	0.2755	0.0883
V_{Gen_12}	1.0071	1.0045	Q_{C_79}	0.1532	0.1751
V_{Gen_15}	1.0202	1.0723	Q_{C_82}	0.1497	0.1252
V_{Gen_18}	1.0075	1.0141	Q_{C_83}	0.2669	0.2266
V_{Gen_19}	1.0171	1.0131	Q_{C_105}	0.0467	0.0452
V_{Gen_24}	0.9646	0.9522	Q_{C_107}	0.2184	0.0081
V_{Gen_25}	0.9453	0.9580	Q_{C_110}	0.1601	0.2947
			$S_{emission}$(ton/h)	**2.4463**	2.5264
			S_{fcost}($/h)	**61912.0100**	62160.8900

$$d_{average} = \frac{1}{n}\sum_{i}^{n} d_i \tag{36}$$

where $d_{average}$, which has a practical reference point, denotes the mean value of all d_i.

B. HV

HV is applied to calculate the super volume of the non-dominant solution set to the real Pareto frontier. Detailed descriptions of HV can be found in [24]. The wider the Pareto front is distributed, the larger the index, which indicates that the relative performance of the solution is better.

$$HV = C_{volume}(\bigcup_{i=1}^{num} v_i) \tag{37}$$

where v_i depicts the volume of the ith individual with a fixed point.

C. Statistical Analysis of Data

The analysis is anchored in 30 simulation tests of IHCSA, CSA, NSGA-II, and MOPSO algorithms.

The SP and HV will be calculated using the data from Case1-8. Besides, calculation results will be presented intuitively using the block diagram.

Box plots can reflect many characteristics of the data, including medians, outliers, etc.

The maximum and minimum data values are at the box's top and bottom, respectively. Meanwhile, the points scattered outside the box represent this data set's outliers. Fig. 17 reveals that the SP data of IHCSA fluctuates less. Compared with the other three algorithms, the average value of the data achieved by IHCSA is lower in most Cases. In Case 2 or Case 3, the SP data of IHCSA is slightly less volatile than the other three methods, but the average value of ones is smaller, and it has no outliers. From the simulation Cases, the Pareto front and BMS obtained by IHCSA are better than the other three algorithms.

Fig. 18 indicates that compared with the other three methods, the HV index of the data gained by IHCSA has less volatility. In most cases, the average value obtained by IHCSA is larger, and the deviation of data is minor. We can consider that the Pareto frontier obtained by this algorithm has great diversity. TABLE XXII and TABLE XXIII depict detailed SP and HV indicators results.

D. Algorithm Time Complexity

If an algorithm can find a quality solution, it requires to consume a lot of time as the cost. Combined, that means the method is not a valuable reference method. This paper uses the average running time to evaluate the time complexity of different algorithms. In practical problems, while an algorithm has excellent performance, the efficiency of solving the problem is also an essential factor for dispatchers to favor the algorithm. TABLE XXIV denotes the average running time of the four algorithms that ran 30 times independently in Case1-10. It is clear from Fig. 19 that compared with CSA, NSGA-II, and MOPSO, the IHCSA takes less time to solve MOOPF problems and is more likely to be favored by decision-makers, so it can be applied to practical engineering problems.

VII. CONCLUSION

In this paper, a novel IHCSA method, which integrates sinusoidal nonlinear transformation awareness probability, tent map switching flight length, and cross mutation mechanism of DE algorithm, is proposed to deal with the MOOPF problem. Various multi-objective models are built up, considering S_{fcost}, S_{VD}, S_{fcost_vp}, $S_{emission}$, and S_{Ploss}.

In the IEEE30-, IEEE57-, and IEEE118-bus test systems, ten cases that satisfy system constraints are applied to detect the applicability of IHCSA. Three multi-objective optimization strategies are combined: SAPM, ENSM, and BMS, to acquire a well-distributed Pareto frontier. Besides, time complexity and two performance evaluation indexes, SP and HV, are applied to test and evaluate the proposed algorithm's performance comprehensively. Through the experimental results, IHCSA has a tremendous advantage and strong competitiveness over MOPSO, CSA, and NSGA-II methods in processing the MOOPF problem.

Consequently, the proposed IHCSA is a selectable approach for treating the MOOPF problem in an actual power system.

TABLE XXII
DETAILS OF SP FOR VARIOUS METHODS

Evaluation Index	Case	Mean(*M*) and Deviation(*D*)	Method			
			IHCSA	CSA	NSGA-II	MOPSO
SP	Case1	*M*	0.8452	0.8042	0.8870	0.7860
		D	0.0964	0.1234	0.0861	0.2418
	Case2	*M*	0.7591	0.8129	0.8198	0.6393
		D	0.0902	0.0554	0.0600	0.2198
	Case3	*M*	0.9327	1.0227	1.0152	0.9231
		D	0.0816	0.1067	0.1100	0.1472
	Case4	*M*	0.0225	0.2558	0.0422	-
		D	0.0215	0.3273	0.0209	-
	Case5	*M*	1.0405	1.0862	1.1284	0.8753
		D	0.1224	0.1332	0.1869	0.2953
	Case6	*M*	0.0001	0.0059	0.0007	0.0015
		D	0.0002	0.0061	0.0004	0.0012
	Case7	*M*	7.6493	25.4970	18.0732	-
		D	14.1809	25.4946	5.2979	-
	Case8	*M*	17.7315	58.6647	41.5369	105.8763
		D	20.4094	41.7436	4.0056	61.6223

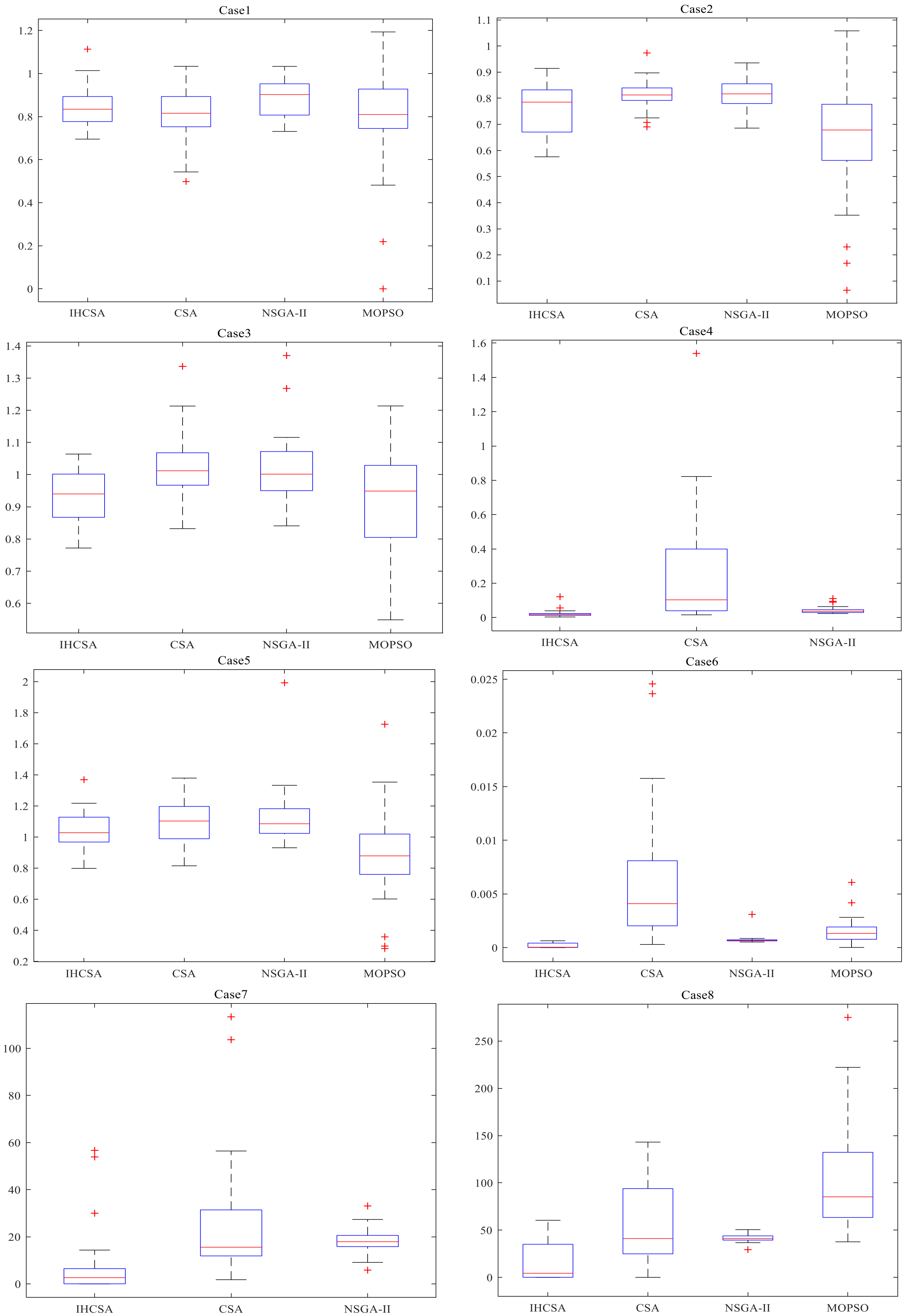

Fig. 17. Boxplots of SP for Case1- Case8

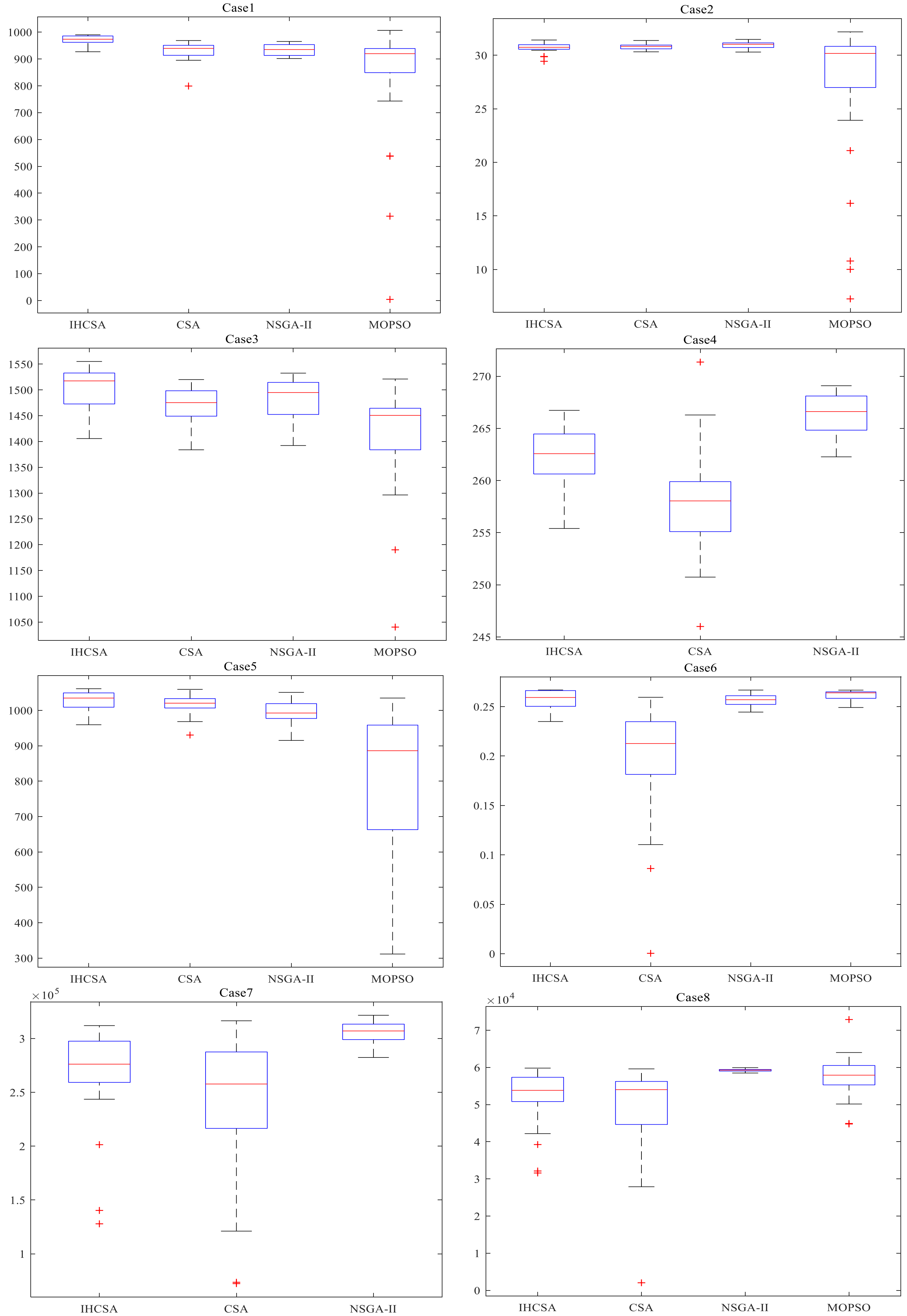

Fig. 18. Boxplots of HV for Case1-Case8

TABLE XXIII
DETAILS OF HV FOR VARIOUS METHODS

Evaluation Index	Case	Mean(M) and Deviation(D)	Method			
			IHCSA	CSA	NSGA-II	MOPSO
HV	Case1	M	973.0801	930.2469	932.8931	834.0144
		D	13.8670	31.9913	20.7314	216.8898
	Case2	M	30.7134	30.8212	30.9592	27.0245
		D	0.41357	0.2781	0.3085	6.81304
	Case3	M	1501.1580	1472.8390	1484.9890	1414.0030
		D	44.0461	32.71222	33.7807	95.6712
	Case4	M	262.4028	257.7612	266.4934	-
		D	2.5497	5.0823	1.8411	-
	Case5	M	1027.1850	1015.7180	991.5192	805.9228
		D	25.9278	25.3616	32.4580	195.7318
	Case6	M	0.2569	0.2005	0.2563	0.2610
		D	0.0095	0.0572	0.0063	0.0054
	Case7	M	267013.5000	240781.1000	305393.4000	-
		D	45366.8600	64731.4800	9425.8480	-
	Case8	M	52259.4200	48947.1500	59239.0900	57802.3000
		D	7393.3220	12206.6900	348.4502	5374.7770

TABLE XXIV
THE MEAN ELAPSED TIME

Method	The Mean Elapsed Time (s)									
	Case1	Case2	Case3	Case4	Case5	Case6	Case7	Case8	Case9	Case10
IHCSA	198.7056	186.3052	189.8382	183.7133	210.4277	183.3281	442.5212	459.8592	1420.4730	1525.8020
CSA	198.3387	182.7500	195.4255	182.9518	208.5639	193.7357	491.5081	485.8934	-	-
NSGA-II	192.3326	185.1319	202.8209	189.5647	214.1398	204.3149	486.3406	529.6825	1555.6238	1485.0140
MOPSO	203.864	202.2720	196.8391	-	210.2265	231.6318	490.5029	502.7455	-	-

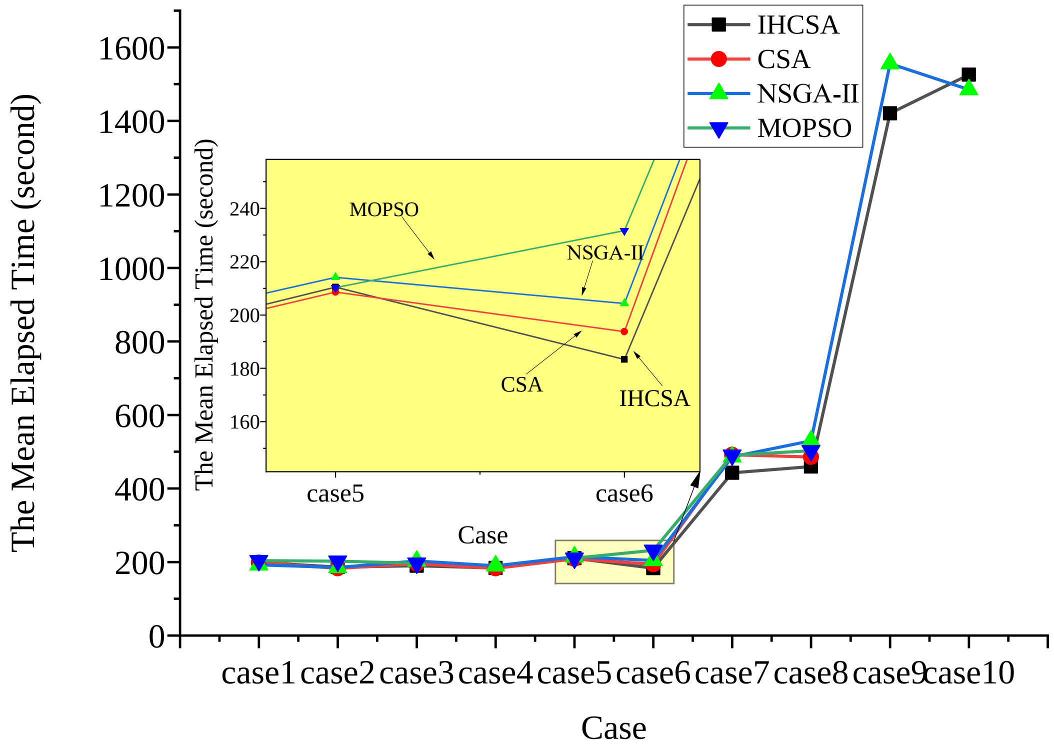

Fig. 19. The mean elapsed time of different algorithms

REFERENCES

[1] H. T. Kahraman, M. Akbel and S. Duman, "Optimization of optimal power flow problem using multi-objective manta ray foraging optimizer," *Applied Soft Computing*, vol. 116, article. 108334, 2022.

[2] H. P. C, K. Subbaramaiah and P. Sujatha, "Optimal DG unit placement in distribution networks by multi-objective whale optimization algorithm & its techno-economic analysis," *Electric Power Systems Research*, vol. 214, article. 108869, 2023.

[3] K. Christakou, D. Tomozei, J. Le Boudec and M. Paolone, "AC OPF in radial distribution networks – Part II: An augmented lagrangian-based OPF algorithm, distributable via primal decomposition," *Electric Power Systems Research*, vol. 150, pp. 24-35, 2017.

[4] Y. Li, C. Wan, D. Chen and Y. Song, "Nonparametric probabilistic optimal power flow," *IEEE Transactions on Power Systems*, vol. 37, no. 4, pp. 2758-2770, 2022.

[5] S. A. El-Sattar, S. Kamel, R. A. El Sehiemy and F. Jurado, *et al.*, "Single- and multi-objective optimal power flow frameworks using Jaya optimization technique," *Neural Computing and Applications*, vol. 31, no. 12, pp. 8787-8806, 2019.

[6] S. B. Pandya, S. Ravichandran, P. Manoharan and P. Jangir, *et al.*, "Multi-objective optimization framework for optimal power flow problem of hybrid power systems considering security constraints," *IEEE Access*, vol. 10, pp. 103509-103528, 2022.

[7] X. Fu, D. Li, H. Wang and J. Yang, *et al.*, "Multi-objective optimization of guide vane closure scheme in clean pumped-storage power plant with emphasis on pressure fluctuations," *Journal of Energy Storage*, vol. 55, article. 105493, 2022.

[8] M. Farahi Shahri and A. Hossein Nezhad, "Multi-objective

optimization to minimize pumping power and flow non-uniformity at the outlets of a distributor manifold using CFD simulations and ANN rapid predictions," *Measurement*, vol. 188, article. 110566, 2022.

[9] Y. Sun, J. Lu, Q. Liu and W. Shuai, *et al.*, "Multi-objective optimizations of solid oxide co-electrolysis with intermittent renewable power supply via multi-physics simulation and deep learning strategy," *Energy Conversion and Management*, vol. 258, article. 115560, 2022.

[10] S. Rahmani and N. Amjady, "Non‐deterministic optimal power flow considering the uncertainties of wind power and load demand by multi‐objective information gap decision theory and directed search domain method," *IET Renewable Power Generation*, vol. 12, no. 12, pp. 1354-1365, 2018.

[11] L. Yin and Z. Sun, "Distributed multi-objective grey wolf optimizer for distributed multi-objective economic dispatch of multi-area interconnected power systems," *Applied Soft Computing*, vol. 117, article. 108345, 2022.

[12] S. Ida Evangeline and P. Rathika, "Wind farm incorporated optimal power flow solutions through multi-objective horse herd optimization with a novel constraint handling technique," *Expert Systems with Applications*, vol. 194, article. 116544, 2022.

[13] Y. S. Mohammed, B. B. Adetokun, O. Oghorada and O. Oshiga, "Techno-economic optimization of standalone hybrid power systems in context of intelligent computational multi-objective algorithms," *Energy Reports*, vol. 8, pp. 11661-11674, 2022.

[14] B. Mallala, V. P. Papana, R. Sangu and K. Palle, *et al.*, "Multi-objective optimal power flow solution using a non-dominated sorting hybrid fruit fly-based artificial bee colony," *Energies*, vol. 15, no. 11, article. 4063, 2022.

[15] A. M. Shaheen, R. A. El-Sehiemy, H. M. Hasanien and A. R. Ginidi, "An improved heap optimization algorithm for efficient energy management based optimal power flow model," *Energy*, vol. 250, article. 123795, 2022.

[16] K. Wang, J. Wang, B. Zeng and H. Lu, "An integrated power load point-interval forecasting system based on information entropy and multi-objective optimization," *Applied Energy*, vol. 314, article. 118938, 2022.

[17] S. Sarhan, R. El-Sehiemy, A. Abaza and M. Gafar, "Turbulent flow of water-based optimization for solving multi-objective technical and economic aspects of optimal power flow problems," *Mathematics*, vol. 10, no. 12, article. 2106, 2022.

[18] R. A. El-Sehiemy, "A novel single/multi-objective frameworks for techno-economic operation in power systems using tunicate swarm optimization technique," *Journal of Ambient Intelligence and Humanized Computing*, vol. 13, no. 2, pp. 1073-1091, 2022.

[19] G. Chen, H. Zhuo, X. Hu and F. Long, *et al.*, "Environment Economic Power Dispatch from Power System Based on Multi-objective Novel Tree Seed Optimization Algorithm," *IAENG International Journal of Computer Science*, vol. 48, no. 4, 2021.

[20] E. Barocio, J. Regalado, E. Cuevas and F. Uribe, *et al.*, "Modified bio‐inspired optimisation algorithm with a centroid decision making approach for solving a multi‐objective optimal power flow problem," *IET Generation, Transmission & Distribution*, vol. 11, no. 4, pp. 1012-1022, 2017.

[21] K. Honghai, S. Fuqing, C. Yurui and W. Kai, *et al.*, "Reactive power optimization for distribution network system with wind power based on improved multi-objective particle swarm optimization algorithm," *Electric Power Systems Research*, vol. 213, article. 108731, 2022.

[22] O. Akdag, "An improved archimedes optimization algorithm for multi/single-objective optimal power flow," *Electric Power Systems Research*, vol. 206, article. 107796, 2022.

[23] J. Sun, J. Deng, Y. Li and N. Han, "A BCS-GDE multi-objective optimization algorithm for combined cooling, heating and power model with decision strategies," *Applied Thermal Engineering*, vol. 213, article. 118685, 2022.

[24] J. Qian, P. Wang, C. Pu and G. Chen, "Joint application of multi-object beetle antennae search algorithm and BAS-BP fuel cost forecast network on optimal active power dispatch problems," *Knowledge-Based Systems*, vol. 226, article. 107149, 2021.

[25] F. Daqaq, S. Kamel, M. Ouassaid and R. Ellaia, *et al.*, "Non-dominated sorting manta ray foraging optimization for multi-objective optimal power flow with wind/solar/small- hydro energy sources," *Fractal and Fractional*, vol. 6, no. 4, article. 194, 2022.

[26] M. El-Dabah, M. A. Ebrahim, R. A. El-Sehiemy and Z. Alaas, *et al.*, "A modified whale optimizer for single- and multi-objective OPF frameworks," *Energies*, vol. 15, no. 7, article. 2378, 2022.

[27] G. Chen, X. Yi, Z. Zhang and H. Wang, "Applications of multi-objective dimension-based firefly algorithm to optimize the power losses, emission, and cost in power systems," *Applied Soft Computing*, vol. 68, pp. 322-342, 2018.

[28] G. Chen, J. Qian, Z. Zhang and Z. Sun, "Multi-objective optimal power flow based on hybrid firefly-bat algorithm and constraints-prior object-fuzzy sorting strategy," *IEEE Access*, vol. 7, pp. 139726-139745, 2019.

[29] J. Qian, P. Wang, C. Pu and X. Peng, *et al.*, "Application of modified beetle antennae search algorithm and BP power flow prediction model on multi-objective optimal active power dispatch," *Applied Soft Computing*, vol. 113, article. 108027, 2021.

[30] L. Liu, Z. Zhang, G. Chen and H. Zhang, "Resource management of heterogeneous cellular networks with hybrid energy supplies: A multi-objective optimization approach," *IEEE Transactions on Wireless Communications*, vol. 20, no. 7, pp. 4392-4405, 2021.

[31] A. Askarzadeh, "A novel metaheuristic method for solving constrained engineering optimization problems: Crow search algorithm," *Computers & Structures*, vol. 169, pp. 1-12, 2016.

[32] D. Gupta, J. J. P. C. Rodrigues, S. Sundaram and A. Khanna, *et al.*, "Usability feature extraction using modified crow search algorithm: A novel approach," *Neural Computing and Applications*, vol. 32, no. 15, pp. 10915-10925, 2020.

[33] A. G. Hussien, M. Amin, M. Wang and G. Liang, *et al.*, "Crow search algorithm: Theory, recent advances, and applications," *IEEE Access*, vol. 8, pp. 173548-173565, 2020.

[34] P. Upadhyay and J. K. Chhabra, "Kapur’s entropy based optimal multilevel image segmentation using crow search algorithm," *Applied Soft Computing*, vol. 97, article. 105522, 2020.

[35] A. M. Anter, A. E. Hassenian and D. Oliva, "An improved fast fuzzy c-means using crow search optimization algorithm for crop identification in agricultural," *Expert Systems with Applications*, vol. 118, pp. 340-354, 2019.

[36] A. Saxena, "An efficient harmonic estimator design based on augmented crow search algorithm in noisy environment," *Expert Systems with Applications*, vol. 194, article. 116470, 2022.

[37] S. Hinojosa, D. Oliva, E. Cuevas and G. Pajares, *et al.*, "Improving multi-criterion optimization with chaos: A novel multi-objective chaotic crow search algorithm," *Neural Computing and Applications*, vol. 29, no. 8, pp. 319-335, 2018.

[38] B. Ji, X. Yuan and Y. Yuan, "Modified NSGA-II for solving continuous berth allocation problem: Using multiobjective constraint-handling strategy," *IEEE Transactions on Cybernetics*, vol. 47, no. 9, pp. 2885-2895, 2017.

[39] K. Deb, A. Pratap, S. Agarwal and T. Meyarivan, "A fast and elitist multiobjective genetic algorithm: NSGA-II," *IEEE Transactions on Evolutionary Computation*, vol. 6, no. 2, pp. 182-197, 2002.

[40] G. Chen, Q. Qin, P. Zhou and P. Kang, *et al.*, "A novel approach based on modified and hybrid flower pollination algorithm to solve multi-objective optimal power flow," *IAENG International Journal of Applied Mathematics*, vol. 51, no. 4, pp. 1-18, 2021.